2020

FLUID INCLUSION STUDY OF SELECTED CALCITE ASSOCIATED WITH NATIVE COPPER, QUINCY MINE, KEWEENAW PENINSULA, MICHIGAN

David Kelly
Michigan Technological University, davidkel@mtu.edu

FLUID INCLUSION STUDY OF SELECTED CALCITE ASSOCIATED WITH NATIVE COPPER, QUINCY MINE, KEWEENAW PENINSULA, MICHIGAN

By

David Kelly

A REPORT

Submitted in partial fulfillment of the requirements for the degree of

MASTER OF SCIENCE

In Geology

MICHIGAN TECHNOLOGICAL UNIVERSITY

2020

This report has been approved in partial fulfillment of the requirements for the Degree of MASTER OF SCIENCE in Geology.

Department of Geological and Mining Engineering and Sciences

Report Co-Advisor:	*Dr. Theodore J. Bornhorst*
Report Co-Advisor:	*Dr. Chad Deering*
Committee Member:	*Dr. John Jaszczak*
Department Chair:	*Dr. John S. Gierke*

Table of Contents

List of figures

Acknowledgements

This report used specimens provided by the A. E. Seaman Mineral Museum. Co-advisors, Drs. Theodore Bornhorst and Chad Deering provided guidance and feedback during this study. I would especially like to thank Dr. Bornhorst for his thorough reviews of my report.

I would like to thank Robert Barron, Department Facilities Manager of Geological and Engineering Sciences, for teaching me to safely operate the laboratory equipment necessary for this study. Thanks are also due to Daniel Seguin for allowing me access to the Materials Science laboratory.

Abstract

The Keweenaw Peninsula is famous for hosting the largest accumulation of native copper anywhere in the world. Previous studies have looked for the fluids responsible for creating the native copper deposits but were unable to conclusively demonstrate that fluid inclusions can provide valuable insight into the hydrothermal/metamorphogenic fluids responsible for these unique deposits.

This report focused on fluid inclusions from calcite precipitated during the native copper mineralizing event. Calcite crystals with inclusions of native copper growing into vugs from a single location, the Quincy Mine, were hypothesized to have a higher chance to be undisturbed by seismic events that would have caused fracturing and leakage of fluid inclusions. Detailed petrographic analysis of the calcite crystals were completed in optical light, SEM, and cathodoluminescence. The calcite was subdivided into three stages consistent with published mineral paragenesis for the Keweenaw native copper deposits: Stage I mostly predated native copper; Stage II was synchronous with native copper formation; and Stage III was a distinct stage after the precipitation of native copper. Fluid inclusions within these 3 stages of calcite were classified as primary, pseudosecondary or secondary and when possible grouped as fluid inclusion families.

Homogenization temperatures ranged from liquid only inclusions (<50°C) to 166°C (uncorrected for pressure), but FIFs of all the stages were found to have inconsistent homogenization temperatures within FIFs. The variability of homogenization temperatures of the fluid inclusions within given FIFs found in this report indicate that they have been affected by post entrapment modification. However, the median homogenization temperatures are believed to approximate the original trapping temperatures. Using median temperature from a Stage I FIF a pressure correction yielded geologically reasonable results.

Salinity within individual FIFs are more consistent than homogenization temperatures suggesting less effect of post-emplacement modification. Within and between families, Stage I ranged from 5.9-18.4 $CaCl_2$ equiv. wt. % (5.0-19.5 NaCl equiv. wt. %). Stage II ranged from 8.9-30.7 $CaCl_2$ equiv. wt. % (7.9-54.9 NaCl equiv. wt. %). Stage III ranged from 0.0-30.5 $CaCl_2$ equiv. wt. % (0.0-49.7 NaCl equiv. wt. %). It is likely that Ca ions were the dominant ions in solution as many of the higher salinity inclusions had final melting temperatures well below what was possible for the NaCl system and had first melting temperatures below -40°C. The large variation in salinity can be explained by the entrapment of variable proportions of high salinity copper-bearing hydrothermal/metamorphogenic fluids with low salinity meteoric waters.

This study also looked at calcite that completely filled the void space it was growing in. It yielded similar petrographic and micro thermometric results as the vug-filling calcite crystals suggesting that non-vug calcite could be used for future studies well.

1 Introduction

Fluid inclusions in hydrothermally precipitated minerals are common in metallic ore deposits. They occur when tiny amounts of the fluid, from which the minerals are precipitating, are trapped in imperfections in the minerals. Fluid inclusions provide a direct way of examining the fluids present during ancient mineralizing events. Since the mid-19th century the study of fluid inclusions has been an essential part of the development of models for the formation of hydrothermal ore deposits (Wilkinson, 2001).

Fluid inclusions can yield very valuable information including the composition, pressure, density, and temperature of the fluids at the time of crystal growth (Goldstein and Reynolds, 1994; Roedder, 1984). Optical microthermometry involves observing phase changes during heating and cooling of fluid inclusions in transparent minerals. These data are used to estimate temperature and the salinity of the fluid. This study applied optical microthermometry to fluid inclusions in calcite samples associated with native copper from the Quincy Mine, Keweenaw Peninsula, Michigan.

The Keweenaw Peninsula hosts the largest accumulation of native copper in the world. Although other districts have produced more copper it is unique in that native copper represents more than 99% of its production (Bornhorst and Mathur, 2017). From 1845 to 1968, mining in the area produced about 11 billion lbs. of refined copper (Weege and Pollack, 1971). The district is historically significant since it was North America's first major mining rush in the 1840s, and by 1880 the native copper mines of the Keweenaw Peninsula were producing 80% of the new copper in the US (Bornhorst and Lankton, 2012).

Despite the fact that the native copper district was a significant producer of copper, published fluid inclusion studies have been limited. The lack of fluid inclusion studies can be attributed, in part, to the fact that the district has been closed for 50 years and it is the only native copper dominated district known in the world. However, the main reason for the lack of fluid inclusion studies can be attributed to conclusions drawn by Livnat (1983) who concluded that fluid inclusions from the Keweenaw Peninsula were largely unsuitable for study because of post emplacement modification. Subsequently, Püschner (2001) investigated fluid inclusions from the Keweenaw Peninsula. Püschner did not specifically address Livnat's (1983) concerns although he considered his results to be valid.

Livnat (1983) used samples for the study of fluid inclusions wherein the minerals completely filled once open spaces. These tightly packed minerals would have been more subject to fracturing during faulting, which is likely synchronous with the formation of the deposits (Bornhorst, 1997). Thus, Livnat's (1983) conclusion that most all fluid

inclusions were subjected to post emplacement modification is reasonable. To minimize post emplacement fracturing, this study focused on well-formed crystals protruding into what is open space today to investigate if fluid inclusions could yield useful insight into the genesis of native copper deposits of the Keweenaw Peninsula.

2 Geologic Setting

The Keweenaw Peninsula native copper district is hosted by the ~1.1 billion-year-old Midcontinent Rift (MCR). The MCR extends more than 2200 km from Kansas through Lake Superior and down through Lower Michigan (Figure 1).

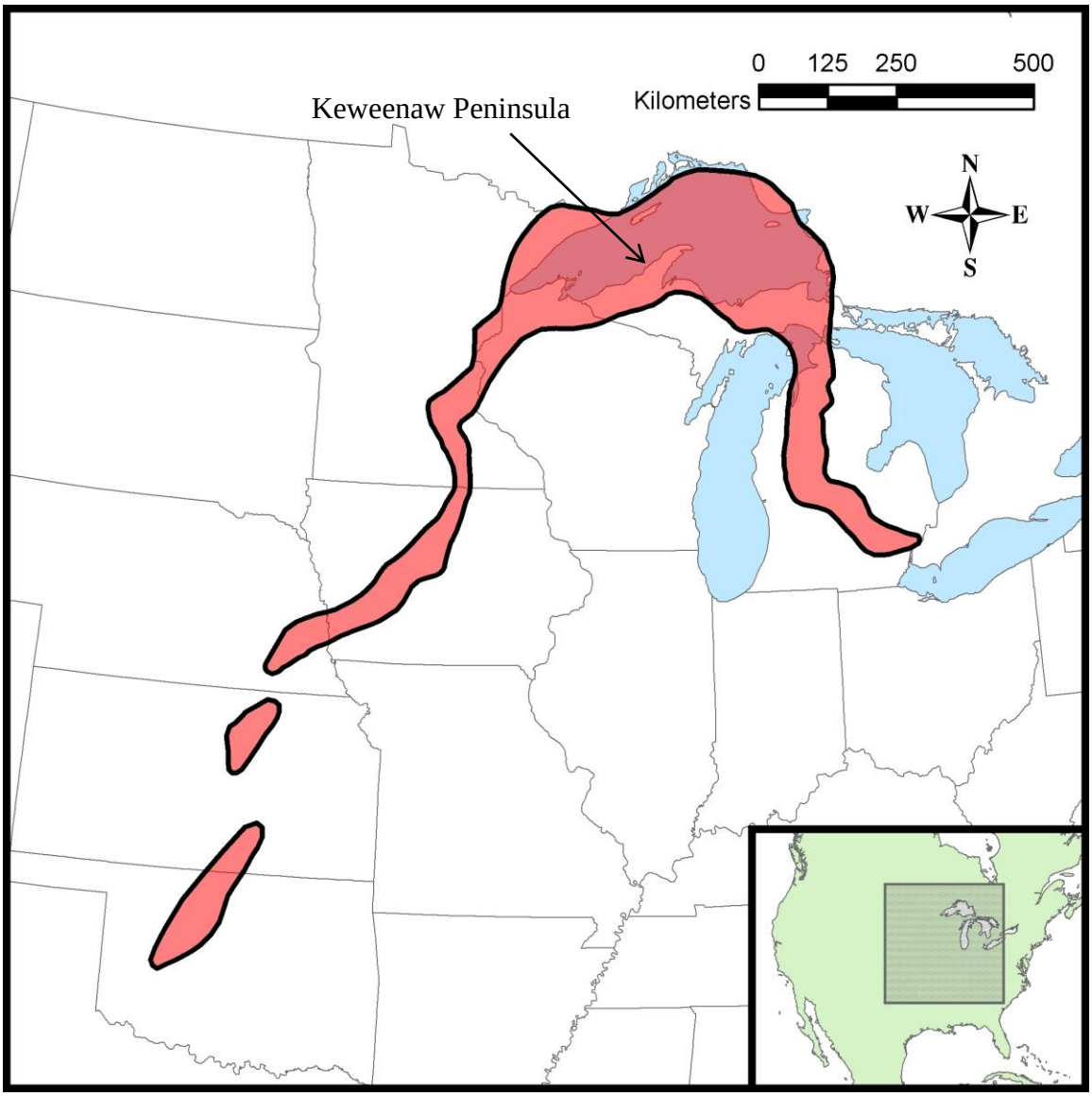

Figure 1. Regional Geology of Midcontinent Rift. The approximate location of the Midcontinent Rift is shown here in red. The Keweenaw Peninsula, the study area, is also indicated on the map. Modified after Cannon (1994).

The Portage Lake Volcanics (PLV) are the main host for native copper. The exposed PLV is over 4.5 km thick on the Keweenaw Peninsula, and the base of the formation is

truncated by the Keweenaw Fault (Figure 2) (Butler and Burbank, 1929). The PLV consists of over 200 subaerial tholeiitic basalt lava flows that range in thickness from less than 1 meter to over 400 meters, with the average lava flow being 10 meters thick (Paces, 1988).

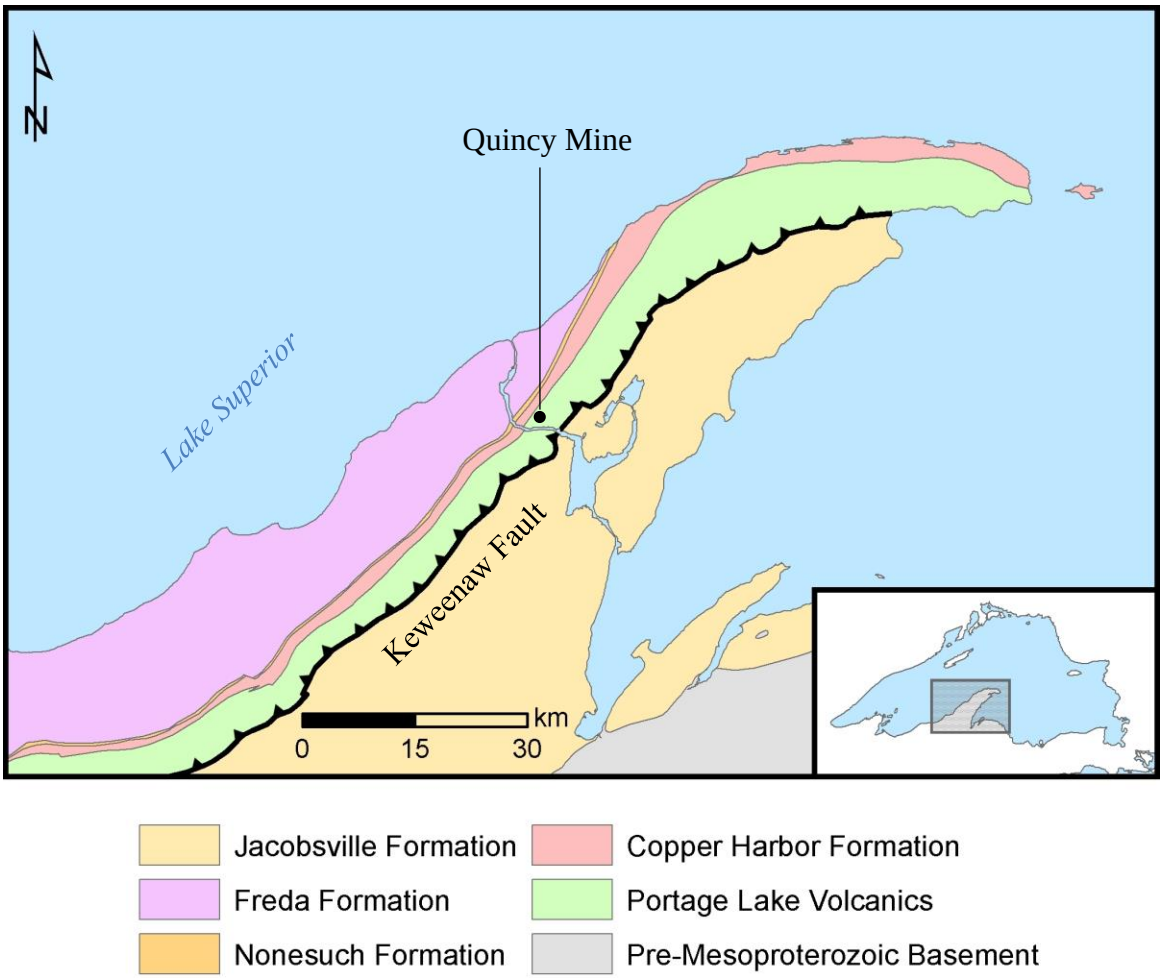

Figure 2. Geologic map of the Keweenaw Peninsula, Michigan. The Portage Lake Volcanics seen here in green and are the main host for native copper.

Major magmatism associated with the rift occurred from 1109 to 1087 Ma with the PLV forming around 1095 Ma over a 2 to 3 million year span (Davis and Paces, 1990). The rift-filling sedimentary units of the Oronto Group followed after major magmatism waned. By 1060 ± 20 Ma reverse faulting began (Cannon et al., 1993). Native copper formation is also thought to have occurred around the same time as reverse faulting 1060 to 1047 Ma (± ~ 20 m.y.) (Bornhorst et al., 1988). The PLV was altered by low grade hydrothermal-metamorphogenic fluids (Jolly and Smith, 1972) which resulted in the

formation of a suite of secondary minerals, including native copper, that filled permeable voids within lava flow tops, interflow sedimentary horizons, and crosscutting fissures. For a more in-depth discussion of the native copper forming event see Bornhorst and Mathur (2017).

2.1 Quincy Mine Hydrothermal-Metamorphogenic Minerals

Native copper at the Quincy Mine was temporally and spatially accompanied by abundant quartz and calcite, along with less abundant epidote, pumpellyite, and chlorite as well as rare prehnite (Bumgarner, 1980; Butler and Burbank, 1929). Laumontite is a late-stage mineral at the Quincy Mine superimposed on top of main-stage minerals at all depths (see Figure 4). Butler and Burbank (1929) also noted that quartz and calcite commonly form crystals in open cavities at shallower depths in the mine and that calcite could be an early-, main-, or late-stage hydrothermal mineral.

The Pewabic lodes, at the Quincy Mine, are known for exceptional calcite crystals with inclusions of native copper making the calcite appear pinkish in color. Palache (1898) described the Quincy Mine calcite crystals as often clear and colorless with an internal growth of native copper that outlines a “shadow crystal”. These “shadow crystals” commonly also had a milky appearance to them which was not commonly found at other deposits in the district. The shadow crystals described by Palache (1898) may represent a paragenetic transition in the growth of the calcite crystals.

3 Previous Fluid Inclusion Studies

Several studies have examined fluid inclusions from the Keweenaw Peninsula native copper district. All of these studies observed fluid inclusions at room temperature which consisted of simple liquid and vapor phases, with the exception of rare daughter minerals in fluid inclusions hosted by quartz (Livnat, 1983; Püschner, 2001). Homogenization temperatures of fluid inclusions in quartz tended to be higher than calcite.

The first study of fluid inclusions from the Keweenaw Peninsula was performed by Donald H. Richter as reported by Stoiber and Davidson (1959). Amygdule-filling quartz and calcite samples were collected from the Kearsarge lode. Homogenization temperatures for quartz ranged from 227-376°C with a median between 295-360°C. Calcite homogenization temperatures ranged from 116-157°C with a median between 133-140°C. The homogenization temperatures for quartz are suspect as they are higher than expected precipitation temperature indicated by hydrothermal-metamorphogenic mineral assemblages (a maximum temperature of ~320°C according to Livnat (1983)). The calcite homogenization temperatures are too low as compared to expected precipitation temperature, but this could be a result of the need to correct the homogenization temperature for pressure of entrapment.

Roedder (1963) recorded the freezing behavior of a single 1 mm long fluid inclusion found in a euhedral calcite crystal containing native copper from the Lake Superior area. The inclusion was reluctant to freeze but did so at -70°C after two days. He observed a first melting temperature around -50°C and a final melting temperature (Tm) of -32.5±1°C and concluded that the brine must have contained salts other than NaCl in considerable amounts, most likely $CaCl_2$.

The next extensive study of fluid inclusions from the Keweenaw native copper district was by Livnat (1983). Livnat (1983) studied fluid inclusions in samples from drill cores, poor rock piles, and some museum quality specimens of quartz and calcite representing 41 different locations. Calcite homogenization temperatures ranged from 63-148°C while quartz ranged from 92-188°C. Of the 123 samples of quartz studied by Livnat (1983) only 4 fluid inclusions were classified by him with any degree of confidence as primary. Livnat (1983) concluded that fluid inclusions in virtually all of his samples were poorly suited for study on the basis of either small size, difficulty in classification, or post-entrapment changes such as necking. No low temperature microthermometry of the fluid inclusions was performed by Livnat (1983).

Richards and Spooner (1986) published an abstract in which they described 550 inclusions within quartz from the Pewabic and Kearsarge lodes. They believed they found a mixing trend with a low temperature low salinity end member (<100°C

homogenization temperatures and ~1.0 equiv. wt. % NaCl) to a high temperature high salinity endmember (homogenization temperatures ~600°C with 21 equiv. wt. % $CaCl_2$).

Schleiss (1986) performed a fluid inclusion study of calcite from the Delaware Mine in Keweenaw County, Michigan. Eleven calcite chips were collected underground from veins in the mine yielding 139 “isolated” and 113 “fracture-controlled” fluid inclusions. His isolated inclusions had homogenization temperatures of 69-341°C with a peak around 110-130°C and another around 220-280°C, while fracture controlled inclusions ranged from 61-215°C. The high degree of variability of homogenization temperatures was consistent with Livnat’s (1983) conclusion that almost all fluid inclusions were subjected to post-emplacement modification.

Püschner (2001) studied fluid inclusions in quartz and calcite from ten drill core samples and 2 samples from the C&H mine. His fluid inclusion studies identified distinct high and low saline fluids that he attributed to the main native copper forming event. For example, in drill cores from the Ahmeek profile calcite was found to have a fluid population of 23 equivalent weight percent NaCl with a homogenization temperature around 157°C and a second population of 6 equivalent weight percent NaCl with homogenization temperatures around 91°C.

4 Sample Selection

A suite of euhedral calcite crystals with inclusions of native copper from the Quincy Mine were donated by the A. E. Seaman Mineral Museum for this study (Figure 3). Twenty-one different crystals were selected to be made into thick sections. At the outset of this study, only euhedral calcite crystals were selected because the crystals were freely growing into vugs that therefore presumably minimized fracturing from seismic events. Selecting calcite with inclusions of native copper helped to ensure that the crystals were precipitated simultaneously with native copper. As the samples were originally recovered for resale and not for scientific study, none of the original locations of the crystals from within the Quincy Mine were recorded. The similarity of all of the 21 crystals to one another suggests they could have come from the same vug which limits the representativeness of the samples. These calcite crystals with included native copper are more likely from less than 165 meters below the surface where such crystals are more common.

After fluid inclusion data were obtained from the calcite crystals, an anhedral open space filling calcite was selected for study from the A. E. Seaman Mineral Museum, Keweenaw research collection. The sample came from the 60th level near the No. 2 shaft, around 1170 meters below the surface, and thus, it was from much deeper in the mine than the euhedral crystals and also not a vug-filling calcite crystal.

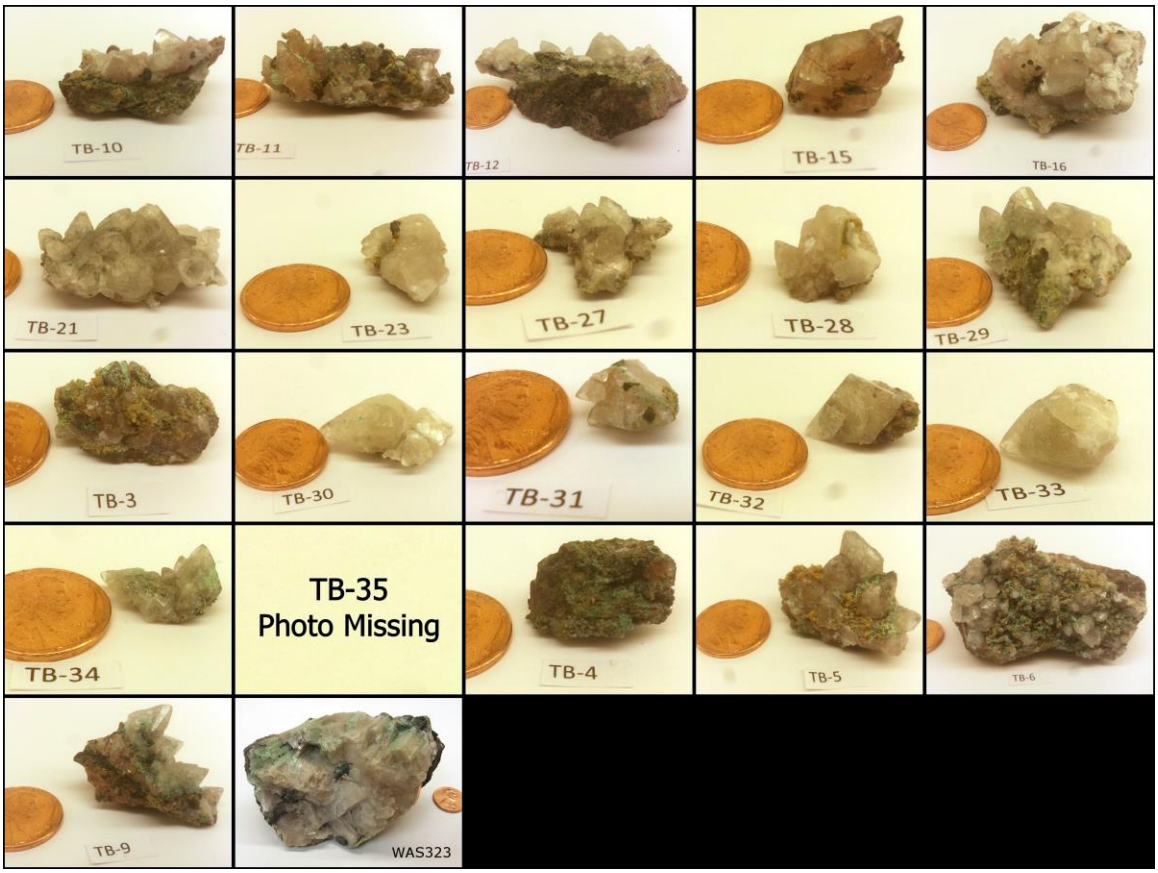

Figure 3. Copper included calcite samples examined in this study. All of them except WAS323 were freely growing into vugs. WAS323 has inclusions of copper and was a massive anhedral calcite that had completely filled the space in which it was growing.

5 Methods

Great care was taken to not overheat or mechanically deform the calcite crystals during preparation for fluid inclusion studies. Since the samples were subjected to different analytical methods, the application of each method was ordered to prevent one analytical method from affecting the results of another.

5.1 Thick Section Preparation and Petrography

Multiple photographs were taken of each calcite sample prior to preparation of thick sections. Thick sections were cut from each crystal perpendicular to the c-axis in order to maximize the time represented by the section while allowing multiple sections. After a rough polish the thick sections were sorted based on their potential for yielding visible primary fluid inclusions. The best sections were doubly polished. After further examination, those doubly polished thick sections with the best chance of yielding primary fluid inclusions were selected for detailed study.

The selected doubly polished thick sections were photographed in both transmitted and reflected light. The images were imported into ArcGIS to generate digital maps. Areas of interest were identified on the maps followed by detailed petrographic and fluid inclusion description. Fluid inclusions were grouped as potentially primary, secondary, and pseudosecondary. Microthermometry was performed using a Linkham heating and cooling stage. Thick sections were broken into fragments for easier microthermometric testing and previously identified inclusions within a given fragment were heated and observed together and not individually. All inclusions in the fragment were checked for a vapor bubble then the temperature was raised one °C. If an inclusion appeared to have lost its vapor bubble then the temperature was lowered to see if the vapor bubble reappeared by slowly regrowing, indicating that it had not homogenized, or if significant undercooling was required resulting in sudden renucleation, indicating that it had homogenized. For fluid inclusions that had no vapor bubble at room temperature the fragment was cooled, but not frozen, in an effort to nucleate a vapor bubble, indicating metastable condition in the fluid inclusion. Heating of the inclusions to determine homogenization temperature always preceded freezing in order to avoid any stretching of the inclusions due to the pressure that could develop from ice formation and to avoid the expansion of ice crushing vapor bubbles since some of the vapor bubbles may not renucleate in such circumstances rendering measuring homogenization temperature impossible. Fluid inclusions were cooled until completely frozen then slowly warmed to observe the last temperature ice was observed at, also known as the final melting temperature. All useful final melting temperatures were found in the presence of a vapor bubble to avoid metastable ice. Salinity calculations for fluid inclusions have only been

calibrated to inclusions with vapor phases and ones without a vapor phase very often present final melting temperatures that are too high.

Fluid inclusions that leaked during microthermometric testing and those that had necks were not considered as they were affected by post entrapment changes.

5.2 Cathodoluminescence and Scanning Electron Microscopy

Cathodoluminescence (CL) provides an image of the sample that can enhance visualization of mineral textures. Samples that underwent microthermometry were then imaged by CL. Van den Kerkhof and Hein (2001) described the effect that cold cathode systems may have on fluid inclusion integrity and for this reason CL was always performed after microthermometry.

Scanning Electron Microscopy (SEM) was used to help confirm the mineral identified by visible light petrography. SEM requires a carbon coating on the doubly polished sample making CL imaging difficult without repolishing. In addition, the electron beam used in SEM can damage fluid inclusions. For these reasons SEM was the final analytical technique applied.

6 Mineral paragenesis

There were a total of 10 separate minerals identified within the samples: adularia, calcite, chalcocite, chlorite, cuprite, green copper oxide, native copper, native silver, pumpellyite, and quartz. Initial observations indicated that there were three stages of calcite consistent with those described by Püschner (2001). Stage I and II are termed main-stage and Stage III is termed late-stage by Bodden (2019) and Figure 4 summarizes the paragenesis of the area well. Stage I calcite formed a very distinct core and is likely the "shadow crystal" described by Palache (1898). In reflected light it always showed strong lamellar twinning that was absent from the other stages of calcite and under CL it was almost entirely devoid of any growth zonation. Stage II calcite enclosed the core and formed a sharp irregular contact that displayed many embayments, which likely occurred from a corrosive event as described by Püschner (2001). This stage of calcite contained inclusions of native copper, often had numerous fluid inclusions, and had a jigsaw-like surface texture under CL. This jigsaw texture is consistent with rapid growth of the calcite as described by (Moncada et al., 2012). The third stage of calcite was often, but not always, present and occurred as a thin outer rim on Stage II calcite. Stage III calcite contained inclusions of chalcocite. Chalcocite nearest the boundary with Stage II calcite had a mossy texture whereas further away from the border the chalcocite had an arborescent texture. Under CL, there was not a distinct transition from Stage II to Stage III calcite. Stage III calcite was visibly zoned and is consistent with slower crystal growth as described by (Moncada et al., 2012). See Figure 5 for visible light petrographic images and Figure 6 for CL images.

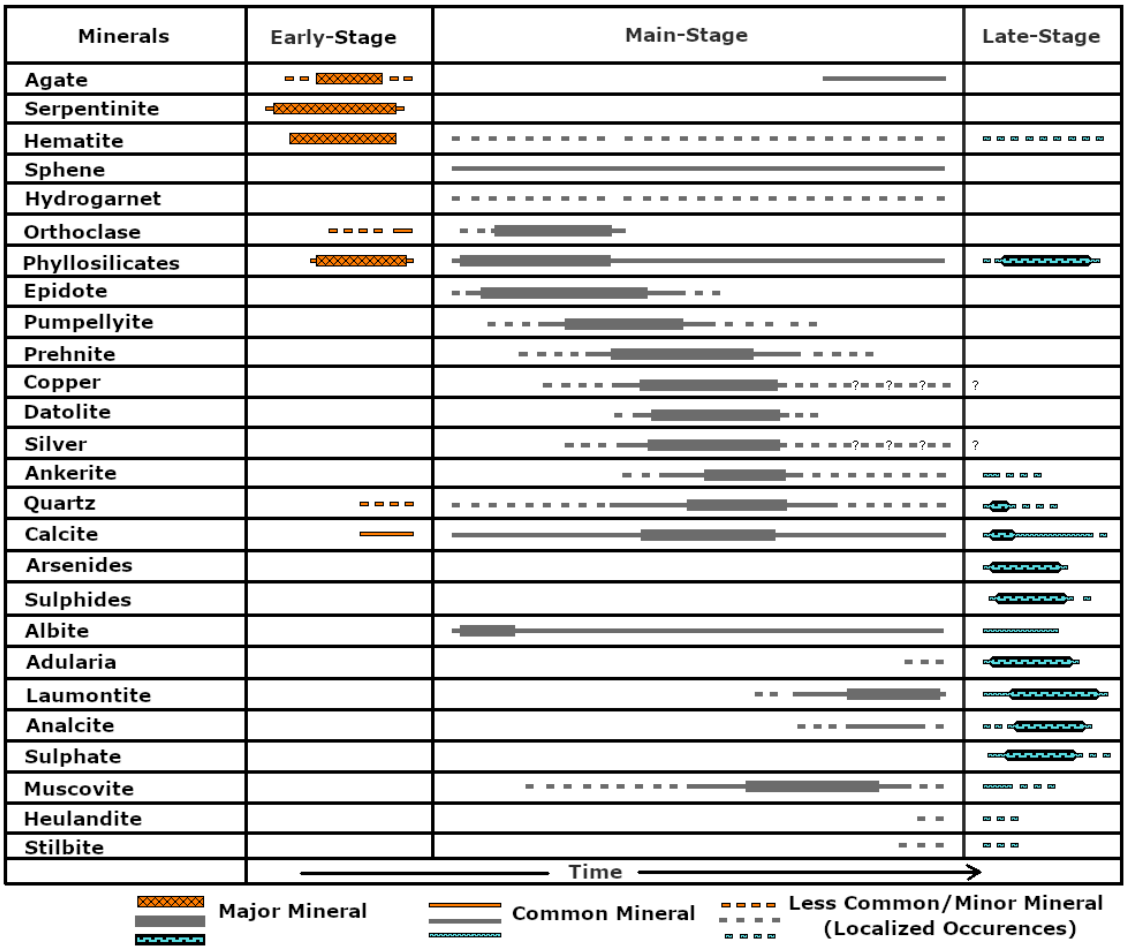

Figure 4. Mineral paragenesis of hydrothermal/metamorphogenic minerals in the Keweenaw Peninsula native copper district and surrounding area. From Bodden (2019) who modified the paragenetic diagram of Butler and Burbank (1929) using data from Jolly and Smith (1971), Livant (1983), and Puschner (2001).

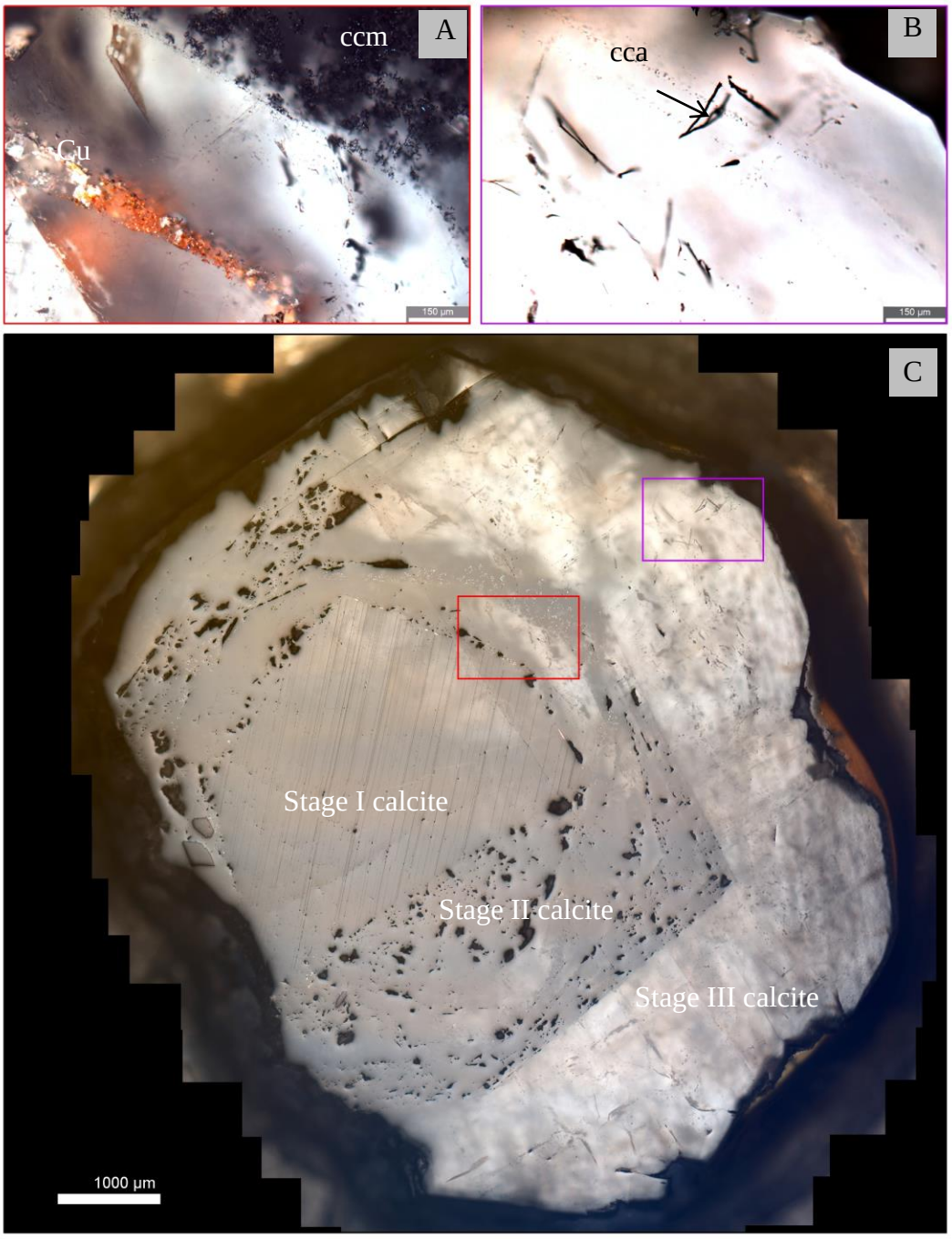

Figure 5. Visible light images of a thick section of a calcite crystal with inclusions of native copper (sample TB-29). A). This inset image shows native copper (Cu) and mossy texture chalcocite (ccm). B) This inset image shows arborescent texture chalcocite (cca). C) This image shows the 3 stages of calcite within the thick section. Inset images were

taken in cross polarized reflected light while the thick section image was taken in plane polarized reflected light.

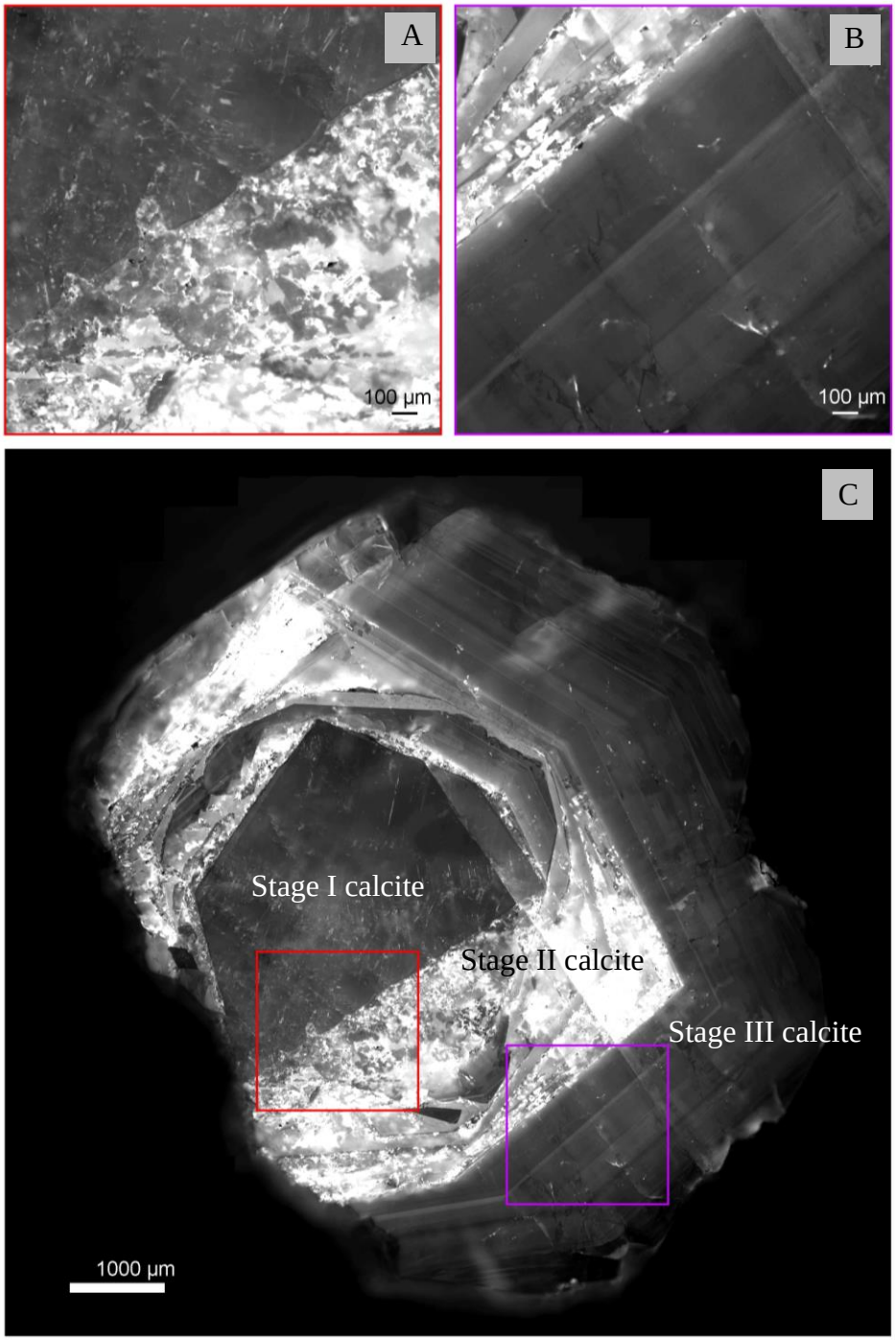

Figure 6. Stages of calcite as visible in CL. A) The red inset image highlights the abrupt and irregular contact Stage I calcite has with Stage II calcite. B) The purple inset

highlights the lack of a visible contact between the jigsaw texture of Stage II and the regular growth zones of Stage III calcite. C) The main image shows the 3 stages of calcite in CL for the thick section. All the color was removed from these images for better viewing.

7 Fluid Inclusion Petrology

In this study, fluid inclusions were classified as primary, secondary, pseudosecondary, or unknown and were grouped into a fluid inclusion family (FIF) whenever possible (Goldstein and Reynolds, 1994; Samson et al., 2003). A FIF is a fluid inclusion assemblage that is interpreted to have formed during a single short interval in time. For example, fluid inclusions that occur continuously along the length of a healed fracture would be grouped together as an FIF. If the fracture terminated within the crystal at a growth zone, the FIF would be classified as pseudosecondary. Secondary FIFs are commonly identified as planar arrays of inclusions that crosscut growth zones and terminate at the crystal surface (Goldstein and Reynolds, 1994). Primary FIFs are best identified by their relationship to growth zones (Goldstein and Reynolds, 1994) but can also be identified through a negative crystal shape or isolation from other fluid inclusions. A pattern of discrepancies in the microthermometric measurements within an FIF is indicative of post entrapment processes such as necking down, stretching, or leakage and refilling (Goldstein and Reynolds, 1994; Samson et al., 2003).

The abundance of fluid inclusions in the Stage I calcite core, varied from extremely crowded to less abundant. In areas that were less abundant in fluid inclusions only pseudosecondary FIFs were identified. Often pseudosecondary FIFs would terminate at the contact with Stage II calcite. In some samples, especially TB-155, pseudosecondary FIFs could be seen radiating from one large fluid inclusion and terminated before reaching the contact. These were interpreted as decrepitation structures and were only found in Stage I calcite. Straight tube-like fluid inclusions at the intersections of lamellar twinning planes were also only found in Stage I calcite, but it is not known how to classify these inclusions, and therefore, they were not tested.

Stage II calcite had numerous fluid inclusions forming a zone around the Stage I calcite core and these were classified as primary. Groups of fluid inclusions within this zone could be seen outlining growth zones that were also isolated from other inclusions; both indicators of primary fluid inclusions. Two Stage II pseudosecondary FIFs that cross-cut Stage I calcite also contained inclusions of native copper and terminated at the Stage I/II calcite contact (Figure 7).

One thick section, TB-155, yielded considerable information on the characteristics of fluid inclusions of Stage II. Numerous fluid inclusions were found in physical contact with native copper which were classified as primary. A pseudosecondary FIF was found that terminated on a Stage II calcite growth zone containing native copper and silver. Fluid inclusions in physical contact with native copper in an otherwise fluid inclusion free area that occurred in reentrants of Stage II calcite cutting into Stage I calcite were classified as primary (Figure 8). Native copper is more abundant on the margins of these reentrants.

In Stage III calcite, primary FIFs outline growth zones and stepped fractures host pseudosecondary FIFs. These fractures were nearby one another and terminated at progressively younger growth zones indicative of sequential fracturing. These stepped fractures often extended from the edge of the crystal face through all of Stage III calcite. Sequential pseudosecondary FIFs seemed to follow truncations in the growth zones, which can only be recognized through CL imaging (Figure 9).

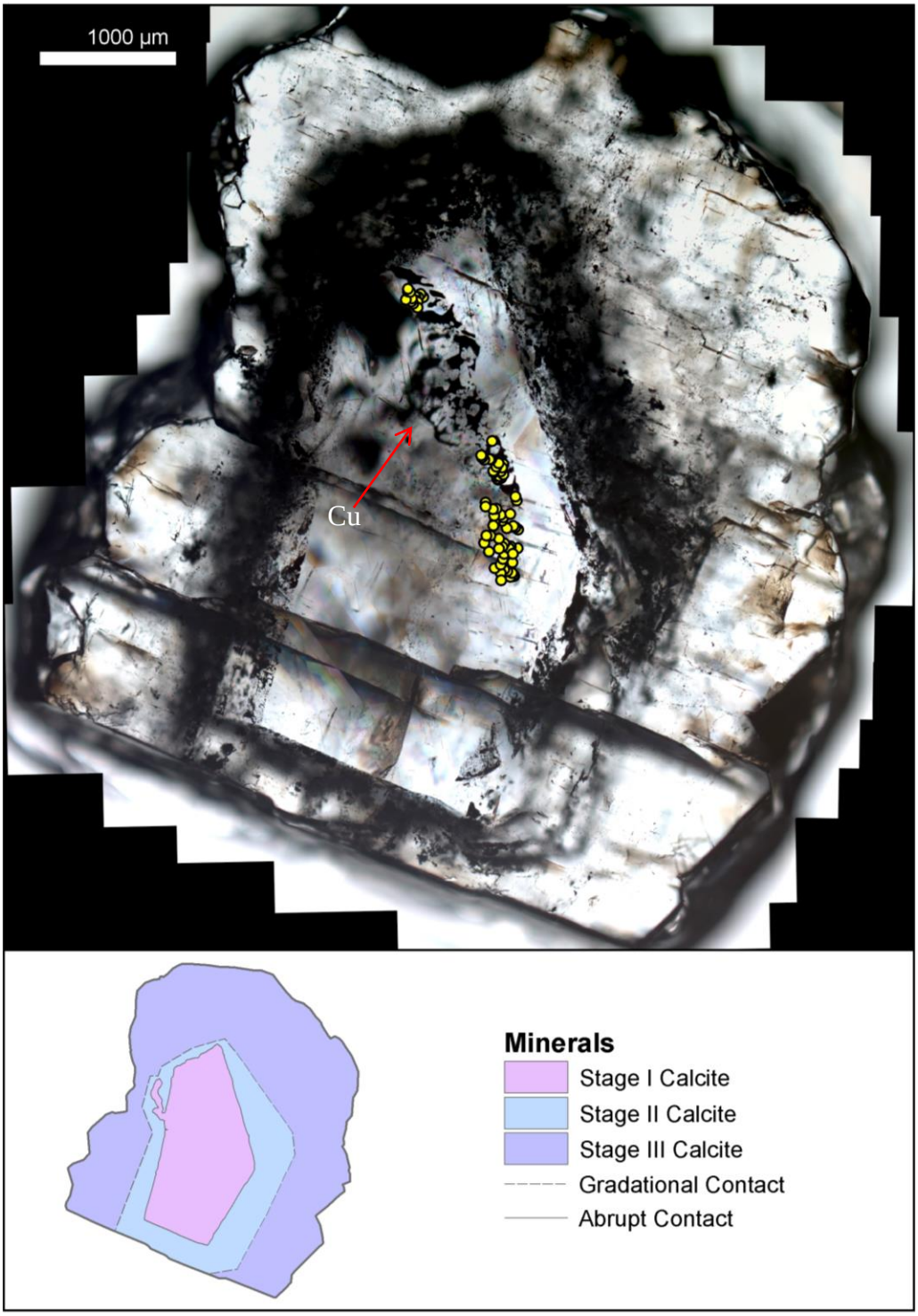

Figure 7. Pseudosecondary FIF with native copper. The red arrow indicates where opaque native copper can be seen in the same orientation as a pseudosecondary FIF while the

yellow circles indicate the fluid inclusions that make up the FIF. This image is a mosaic taken in plane polarized transmitted light.

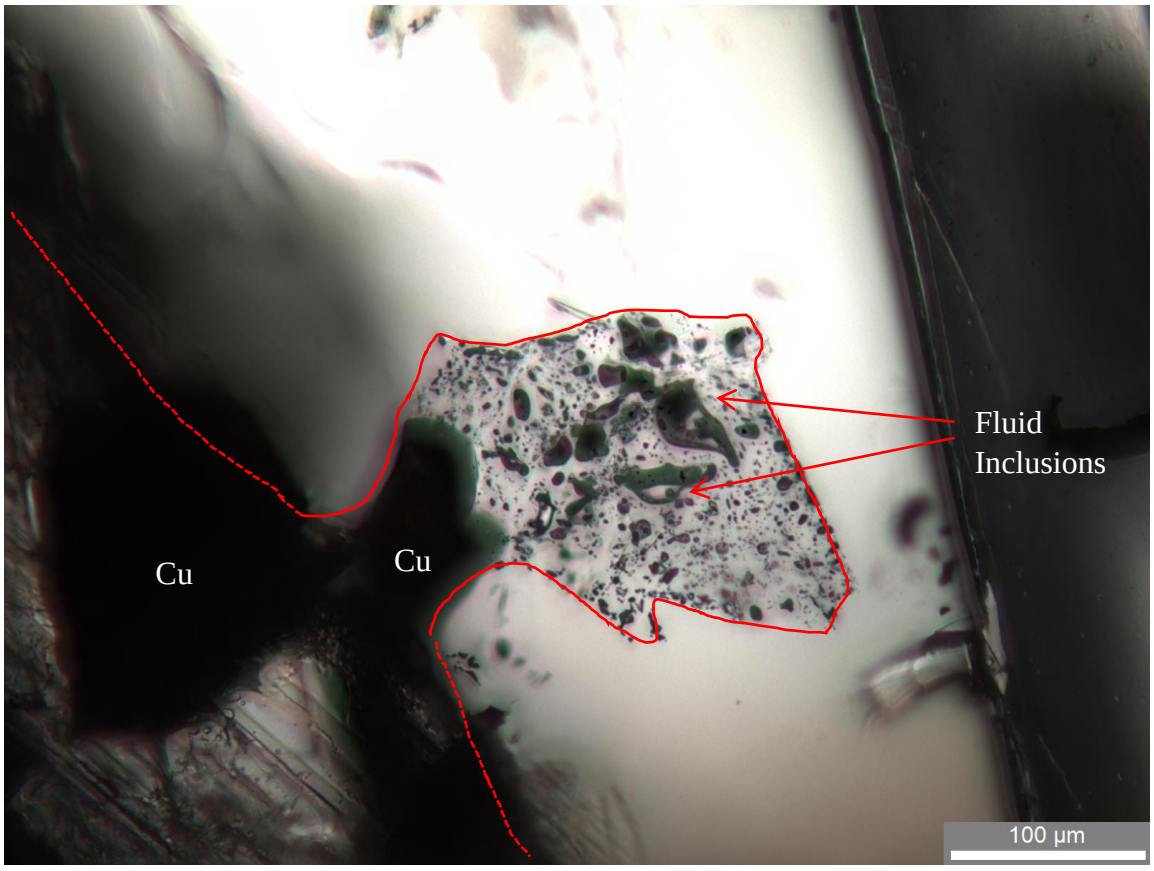

Figure 8. Native copper with primary fluid inclusions. This structure in Stage II calcite contains native copper, fluid inclusions, and calcite and is FIF TB-155-A19. The opaque blebs are native copper and the red arrows show where 2 large fluid inclusions contacting blebs of native copper can be seen. This structure is completely hosted within Stage II calcite. This is a series of 12 photos taken in transmitted plane polarized light composited together with a technique called focus stacking.

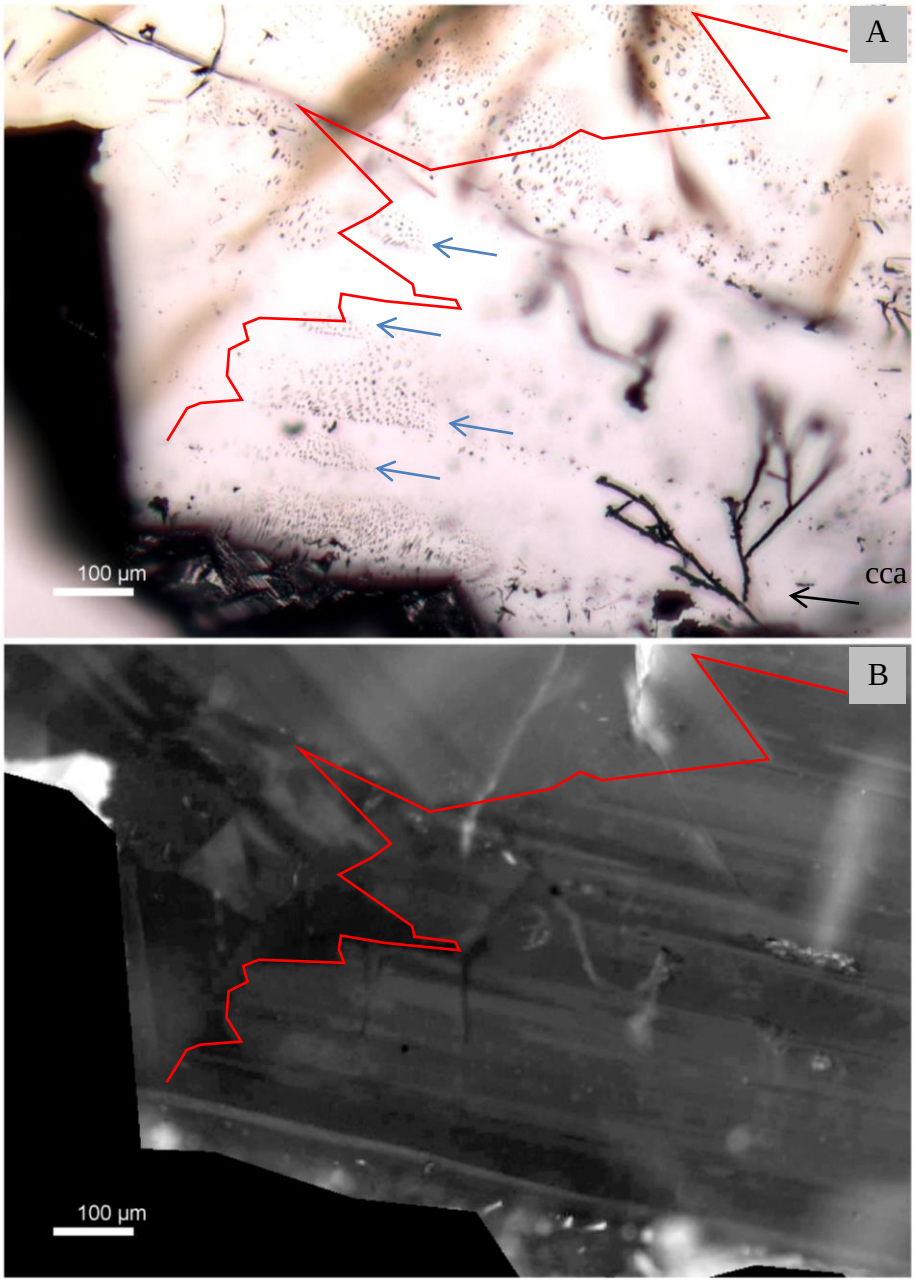

Figure 9. Stepped pseudosecondary FIFs of Stage III calcite in TB-53. A) At first glance these FIFs indicated by the blue arrows may seem like primary FIFs. However, they are indeed planar and terminate on growth zones thus they are classified as pseudosecondary FIFs. The area shown is late Stage III calcite and arborescent texture chalcocite (cca) can be seen near the edge of the crystal. This image was made from a series of 13 photos taken in transmitted PPL composited together with a technique called focus stacking. B) This image taken in CL shows the same area with truncations in the growth zones

outlined in red. The area of truncations aligns well with the stepped pseudosecondary FIFs.

8 Homogenization Temperatures from Calcite Crystals

Homogenization temperatures for individual fluid inclusions ranged from less than 50°C to 166.0°C (Figure 10). A fluid inclusion with no vapor bubble indicates temperatures of less than 50.0°C (Goldstein and Reynolds, 1994) and these are shown as between 35°C and 40°C. Only fluid inclusions that could be classified with reasonable certainty as primary or pseudosecondary and attributed to one of the stages of calcite are shown in Figure 10.

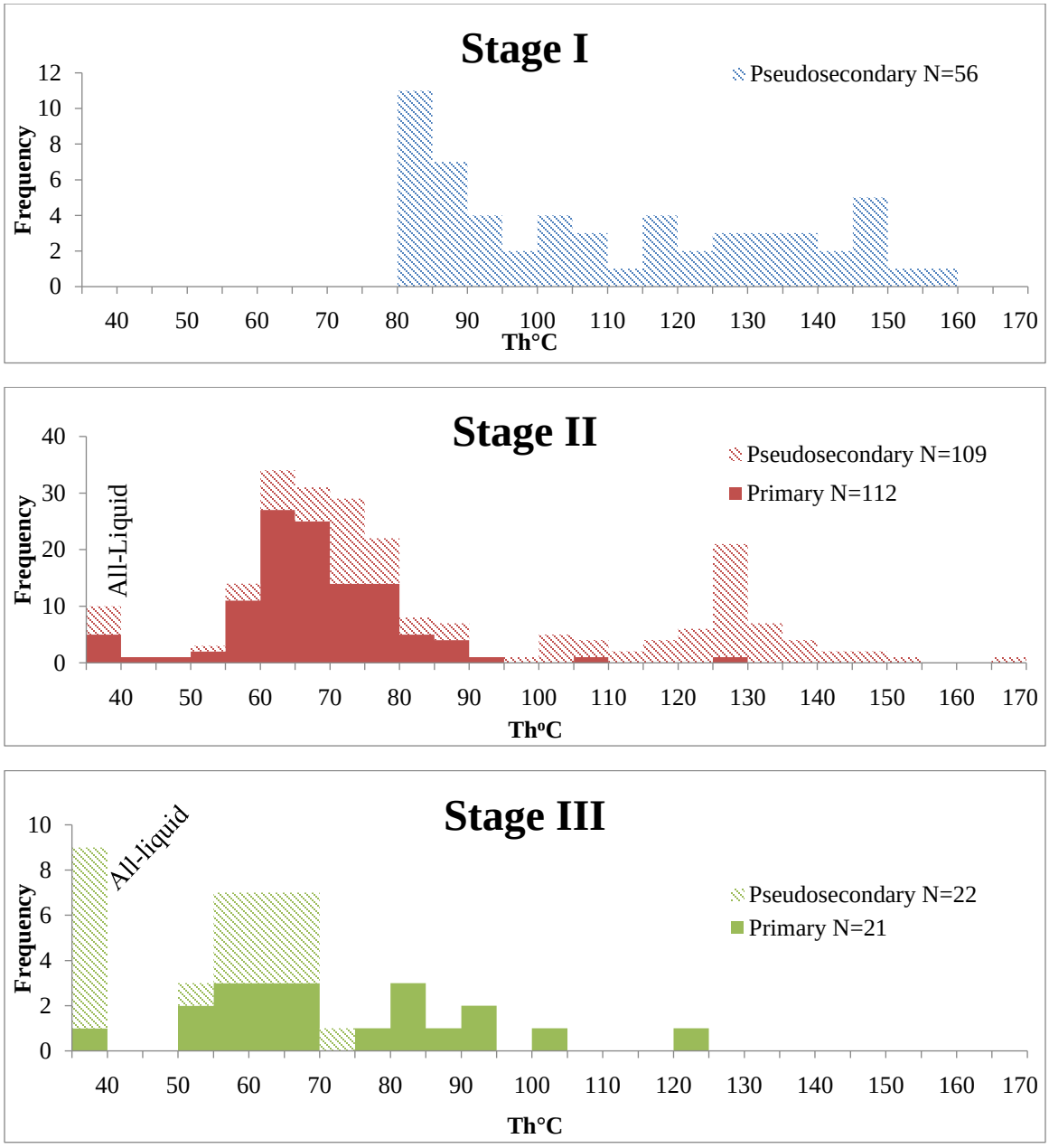

Figure 10. Homogenization temperatures of primary and pseudosecondary fluid inclusions divided into 3 stages of calcite. Note: these histograms are potentially biased because fluid inclusions from an FIF were plotted as individual distinct measurement of points in time whereas the FIF actually represents a short (single) interval of time.

8.1 Consistency of Homogenization Temperatures

Goldstein and Reynolds (1994) considered a FIF to be consistent as long as 90% of the inclusions of variable size and shape fell within a 10 to 15°C interval. The closest any FIF came to meeting these criteria was TB-112-1-A5 for which 85% of the homogenization temperatures fell within 15°C of each other (Figure 11). Thus, homogenization temperatures presented here are not consistent within a FIF. The most obvious explanation for the lack of consistency is post-emplacement modification. There are multiple all liquid fluid inclusions located very close to fluid inclusions with larger vapor bubbles. The all-liquid inclusions could have leaked losing their vapor bubble. Alternatively, the larger vapor bubbles and all liquid inclusions could be due to necking down where the bubble ended up in one part and all liquid in the other. Inconsistency of Stage I FIFs could be due to overheating, as petrographic evidence shows decrepitation structures. This overheating event likely would have occurred after the growth of Stage I calcite but before the growth of the main stage copper event of Stage II.

The lack of consistency is in part or totally explainable by post-emplacement modification. However, the median homogenization temperatures are believed to approximate the original trapping temperature.

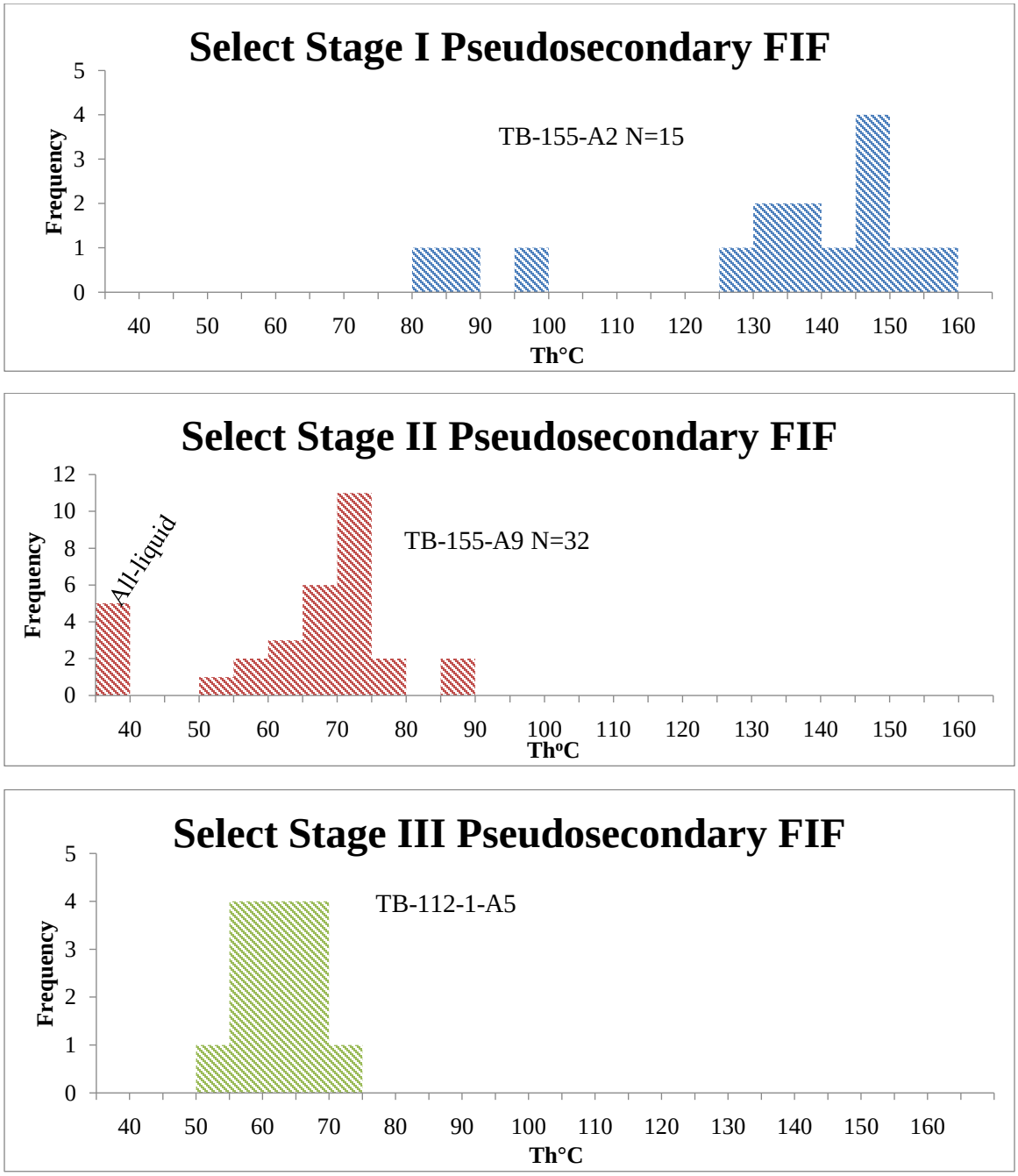

Figure 11. Selected FIFs for homogenization temperatures. These 3 FIFs from the 3 stages of calcite growth show the scatter of homogenization temperatures indicative of lack of consistency.

Fluid inclusion homogenization temperatures are only considered a minimum temperature of entrapment and require a pressure correction to estimate the true entrapment temperatures, which results in higher temperatures. To help determine if the homogenization temperatures are reasonable, a pressure correction can be applied to see if the new temperatures and pressures are geologically reasonable. In this study, all of the fluid inclusions were below the expected temperature of mineralization. This would mean a pressure correction could potentially raise the homogenization temperatures to a geologically reasonable estimate of entrapment temperatures.

Livnat (1983) calculated the maximum temperatures possible for the PLV to be $\lesssim$ 320°C at the exposed base of the PLV with temperatures likely $\gtrsim$150°C near the middle of the overlying Copper Harbor Formation, which he based on phase equilibrium and thermodynamic modeling of mineral assemblages, fluid inclusion filling temperatures, and oxygen isotope thermometry of coexisting silicates. Bornhorst and Rose (1994) compiled data from Livnat (1983), Stoiber and Davidson (1959), and Bornhorst and McDowell (1992) to further constrain the maximum temperature of the Quincy Mine to 210°C $<$ T $<$ 260°C with somewhere around 225°C the most likely temperature.

To apply the pressure correction, the trapping and homogenization temperatures must be known as well as the fluid density. Potter (1977) has provided a means to do this with a series of pressure correction diagrams for salinities up to 25 equiv. wt. %. As Stage I had FIFs closest in homogenization temperatures to the expected maximum temperature of the Quincy Mine, and easily estimated salinities, it was the best choice to apply a pressure correction to. Stage I FIF TB-155-A2 had a median homogenization temperature of 140.0°C. The median final melting temperature of -5.0°C equates to a salinity of 7.9 NaCl equiv. wt. % based on Bodnar (1993) charts. A 10 wt. % NaCl chart from Potter (1977) was used (it was closest to this salinity) to correct the homogenization temperature to a presumed trapping temperature between of 210°C and 260°C. The result of correcting 140.0°C to the expected trapping temperature range of the Quincy Mine at 10 wt. % NaCl equivalent requires pressures between 75 MPa and 140 MPa (Figure 12).

Livnat (1983) inferred pressures of around 50 MPa from the middle of the Copper Harbor Formation based on the stable assemblage of laumontite + quartz, and 150 MPa near the exposed base of the PLV based on the maximum value of the quartz inclusion isochores. Jolly and Smith (1972) theorized total pressure at the base of the exposed PLV was probably between 200-400 MPa during alteration, and also hypothesized that fluid pressures were probably less than total pressure during metamorphism. Based on the maximum thicknesses of the Copper Harbor Formation, Nonesuch Formation, and the Freda Formation provided in Daniels (1982) and the stratigraphic position of the Quincy Mine within the PLV, lithostatic pressure of about 160 MPa could be expected. Based on the measured thicknesses from a USGS cross section through the No. 6 shaft of the

Quincy Mine, lithostatic pressure was calculated to be around 140 MPa, assuming that the Freda Formation was at a maximum thickness of 3660 meters during maximum burial. Price and McDowell (1993) thought the Freda was around 3 km which would have resulted in a pressure around 125 MPa at the Quincy Mine. These pressure estimates are consistent with those derived from the fluid inclusion homogenization temperatures for Stage I calcite. On this basis, despite the lack of consistency, the median homogenization temperatures are approximately valid.

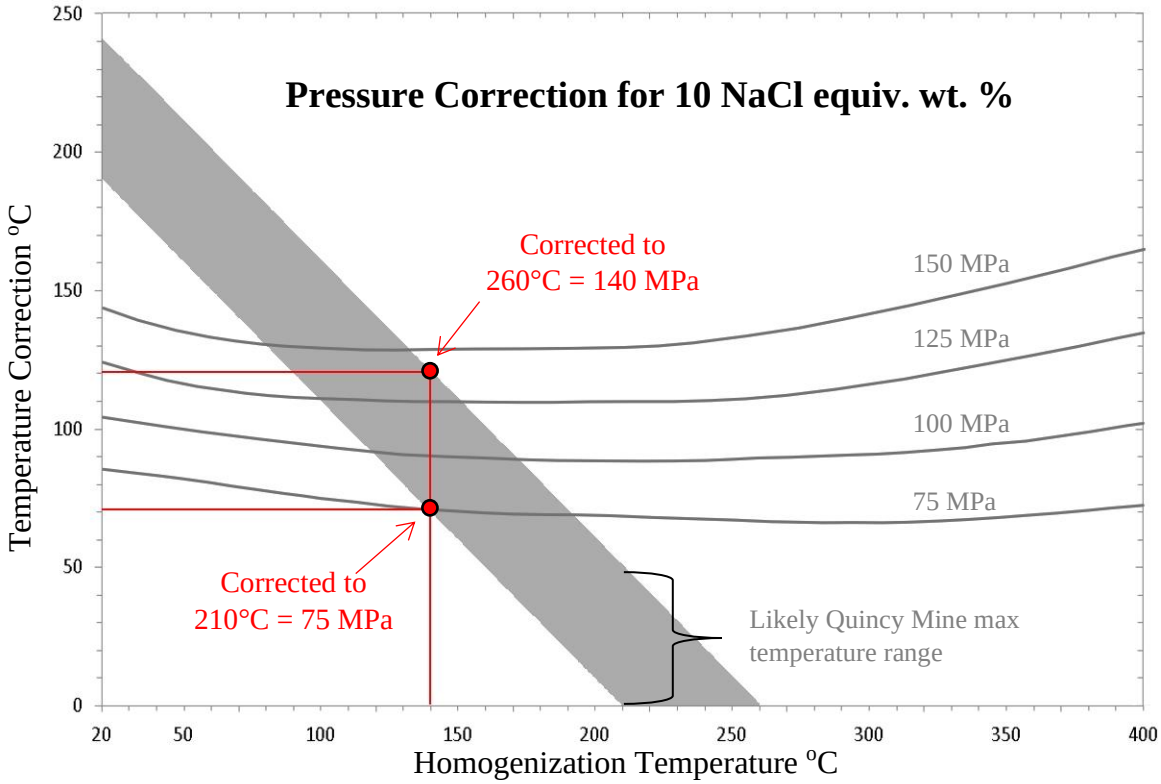

Figure 12. Pressure correction for Stage I FIF TB-155-A2. Stage I FIF TB-155-A2 had a median homogenization temperature of 140.0°C and a calculated median salinity a little under 10 NaCl equiv. wt. %. Correcting this FIF to the likely maximum temperature range of the Quincy Mine yielded pressures of around 75-140 MPa, which seems within reasonable geologic constraints. This diagram has been modified from Potter (1977) and shows the likely Quincy Mine maximum temperature range as a gray zone. Starting at the homogenization temperature on the x-axis a vertical line can be drawn to any point within the gray zone to find the needed temperature correction on the y-axis. The x,y coordinate of the point also shows the likely corresponding pressures during the time of entrapment.

9 Final Melting Temperature from Calcite Crystals

Salinities for Stage I ranged from 5.0 to 19.4 NaCl equiv. wt. % (5.9 to 18.4 $CaCl_2$ equiv. wt. %), which is equivalent to final melting temperatures of -3.0°C to -16.0°C. Fluid inclusions of Stage II had a single solid phase, two distinct solid phases, or metastable solid assemblages upon freezing depending on the rate of warming after freezing. Stage II FIFs with a single solid phase upon freezing had salinities range from 8.9 to 30.7 $CaCl_2$ equiv. wt. % (final melting temperatures from -54.0°C to -5.0°C). For inclusions that had two solid phases at low temperatures, the first solid phase had a high relief with final melting temperature between -35.0°C and -30.0°C and the second solid phase had low relief with a final melting temperature between -29.0°C and -5.0°C (Figure 13). These inclusions had final melting temperatures below what is possible for a pure NaCl system and were at minimum 23.2 $CaCl_2$ equiv wt. % (23.2 NaCl equiv wt%) (Goldstein and Reynolds, 1994). Only one FIF, TB-155-A19, was found with metastable solid assemblages of either a single phase or two solid phases depending on the rate of warming after initial freezing. Some fluid inclusions were also unable to be frozen as well within Stage II and were assumed to have very high salinity.

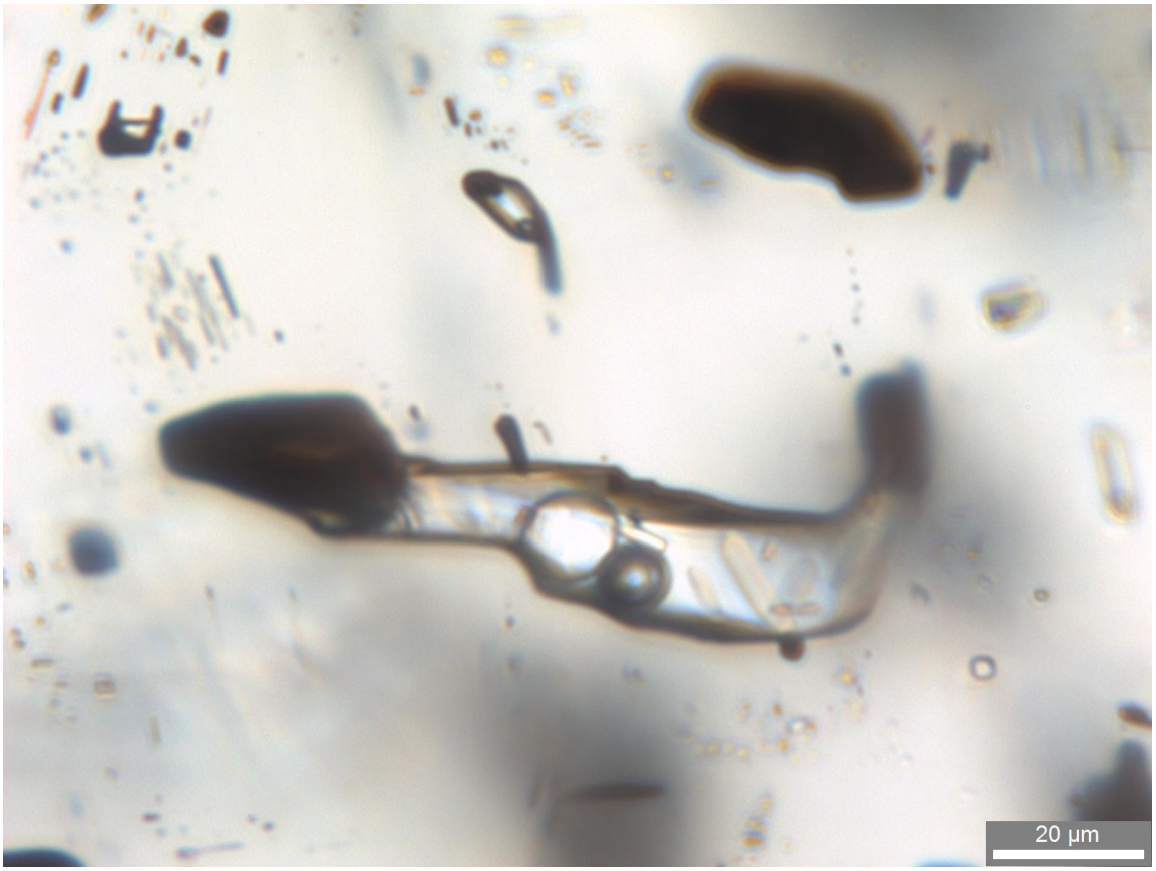

Figure 13. Two solid phases at -36.5°C in in thick section TB-155 fluid inclusion of Stage II. In this image the opaque minerals are native copper with a fluid inclusion in contact with them. This image is representative of other fluid inclusions contacting native copper. The high relief phase was usually rounded and reacted to temperature change quickly, while the low relief phase usually occurred as slightly yellow 6-sided crystals that appeared flat and did not respond quickly to temperature change.

Fluid inclusions of Stage III had salinities from no salinity at all to 49.7 NaCl equiv. wt. % (0.0 and 30.5$CaCl_2$ equiv. wt. %) which is equivalent to final melting temperatures between 0.0°C and -51.0°C (Figure 14). FIFs in early Stage III calcite near mossy texture chalcocite had higher salinities than FIFs in later calcite that contained arborescent texture chalcocite (Figure 15).

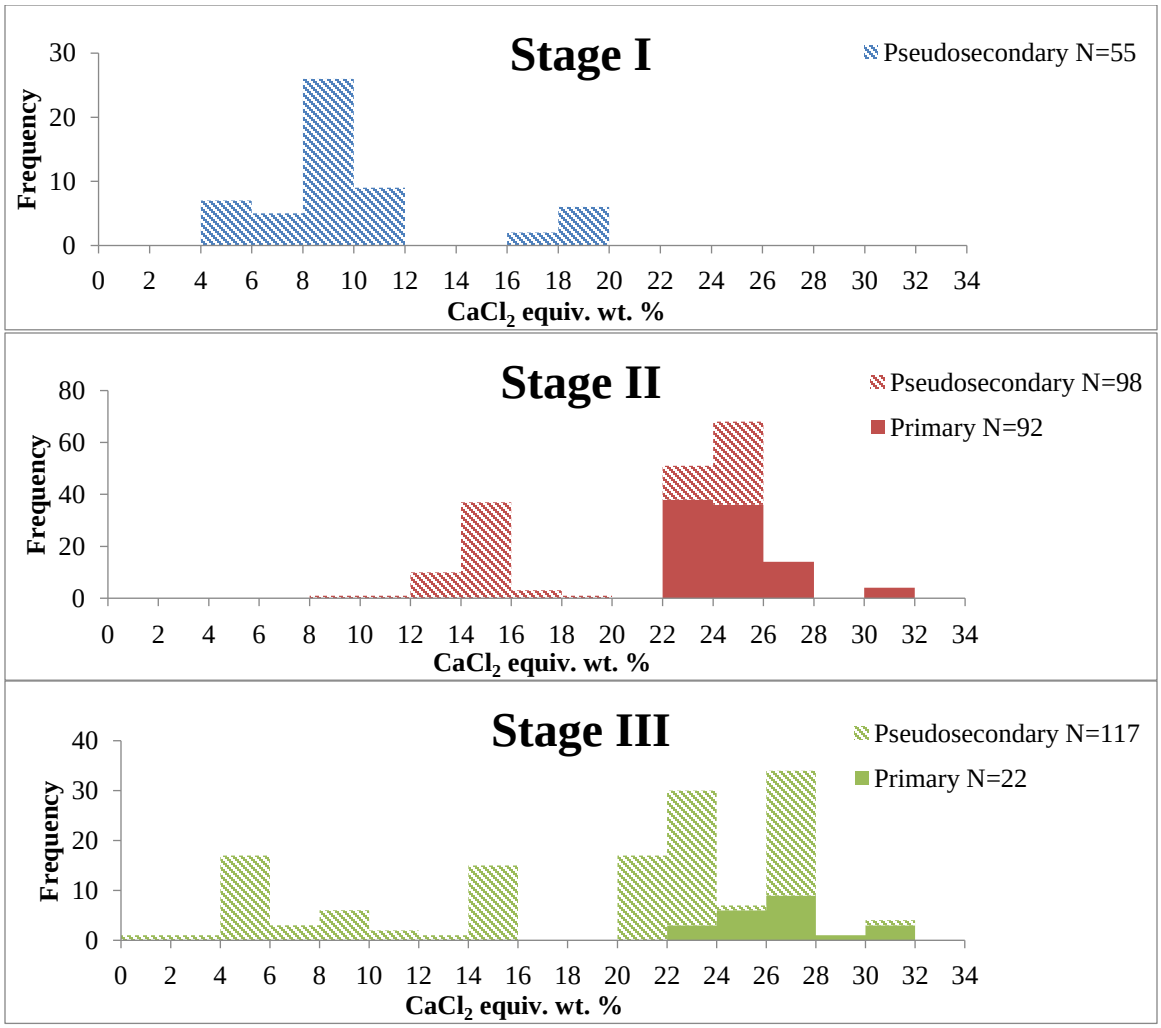

Figure 14. Salinity of fluids in fluid inclusions based on final melting temperature divided into 3 stages of calcite. Salinity is expressed as $CaCl_2$ although there is also likely NaCl in the fluids. Note: these histograms are potentially biased because fluid inclusions from an FIF were plotted as individual distinct measurement of points in time whereas the FIF actually represents a short (single) interval of time.

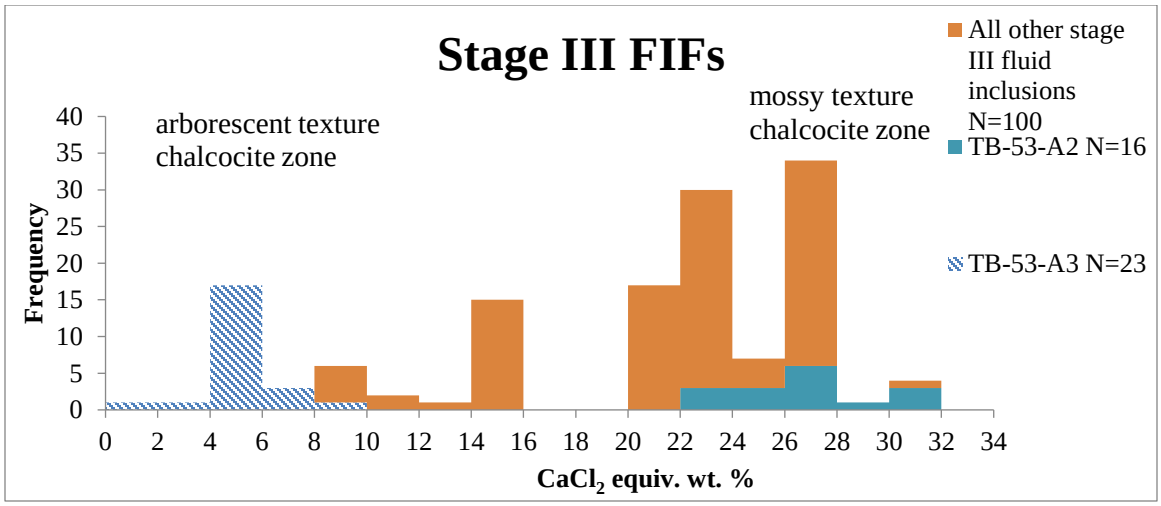

Figure 15. Selected FIFs of late and early Stage III. In this figure FIFs from the earlier mossy texture chalcocite zone (represented by FIF TB-53-A3) are compared to the later FIFs from the arborescent texture chalcocite zone (represented by FIF TB-53-A2). All other fluid inclusions between the arborescent and mossy texture chalcocite zone are represented in orange. Salinity is expressed as $CaCl_2$ although there is also likely NaCl in the fluids, NaCl equivalent salinity is about 62% larger at the highest salinity.

9.1 Consistency of Melting Temperature

For this study, as temperature measurements had an error of 1.0°C, if ≥ 90% of the fluid inclusions within an FIF fell within ±3°C of each other for final melting temperatures (a max salinity range of 4.96 wt.%) they were considered to be consistent.

Four Stage I FIFs with at least five fluid inclusions were consistent. Five Stage II FIFs with at least five fluid inclusions were consistent. Seven Stage III FIFs with at least five inclusions were consistent. The data presented in Figure 14 includes all melting temperature data regardless of whether or not it was consistent and is biased because the number of inclusions representing a FIF is variable. A single FIF represents a single precipitation event and should be represented by only one median melting temperature or salinity. Figure 16 displays consistent and inconsistent FIFs with at least five fluid inclusions along with their median estimated salinities.

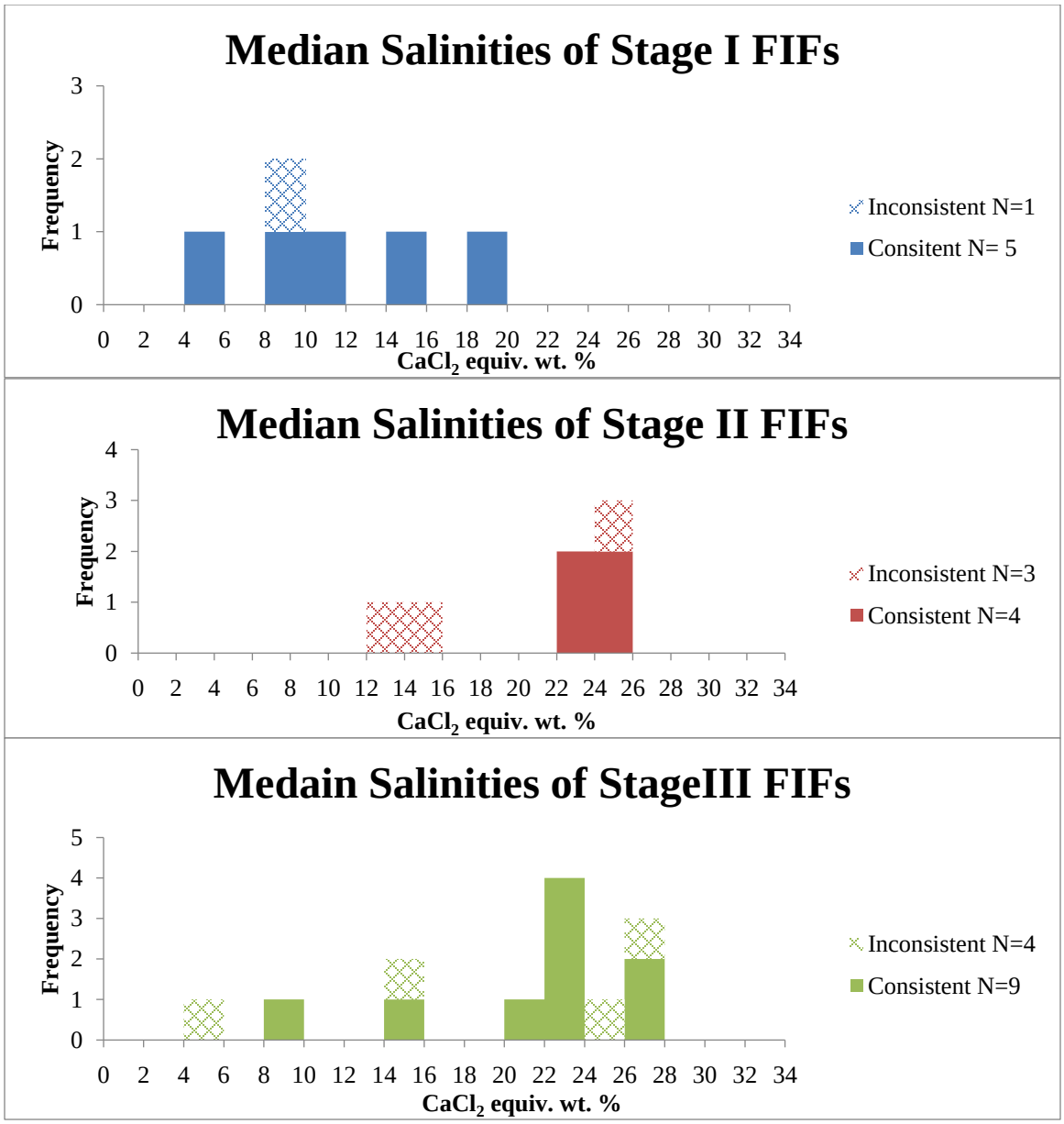

Figure 16. Comparison of median final melting temperatures of the different FIFs whose measurements were consistent and inconsistent. This figure shows the number of consistent vs inconsistent FIFs for each stage. Only FIFs with more than 5 fluid inclusions are shown. A single FIF represents a single precipitation event and is best represented with a central tendency number. Salinity is expressed as $CaCl_2$ although there is also likely NaCl in the fluids, NaCl equivalent salinity is about 27% higher at the greatest salinity.

10 Interpretations of Microthermometry Results

10.1 Composition of Fluids Based on Low Temperature Microthermometry

The freezing point depression is controlled by the salinity of the fluids and is usually expressed as equivalent NaCl although other cations can contribute to the salinity. The type of major ions in the fluids within fluid inclusions can be inferred from the characteristics of melting. The lowest final melting temperature that can be reached by the NaCl-H_20 system when no daughter minerals are present is -21.2°C (Goldstein and Reynolds (1994) and thus, at melting temperatures of this degree or lower other cations must be present in significant quantities. Goldstein and Reynolds (1994) demonstrated that when the first melting temperature is below -40°C the H_2O-NaCl-$CaCl_2$ system should be used to model salinity of the fluids. Use of this system is supported by metastable solid assemblages in some frozen fluid inclusions as the H_20-NaCl-$CaCl_2$ system is also notorious for producing metastable assemblages (Davis et al., 1990; Spencer et al., 1990). The lowest final melting temperature of this study, -54.0°C, would equate to a nearly 100% $CaCl_2$-H_2O system and an estimated salinity of ~ 31 wt. % based on the experimental data of Oakes et al. (1990). The presence of a significant amount of $CaCl_2$ in the fluids is consistent with Livnat (1983) who found high Ca in analyzed fluids derived from the crushing of samples.

Stage I fluid inclusions may have either Ca and/or NaCl the principal cation in the fluid, as the first melting temperatures were difficult to observe. Without a clear first melting temperature below -40°C it is difficult to conclusively demonstrate the major cation. However, the NaCl and $CaCl_2$ systems yield similar levels of salinity so representing the fluids as $CaCl_2$ or NaCl results in approximately the same salinity. Stage II is likely best represented by Ca rich brines as is the early Stage III fluid inclusions as first melting temperatures were typically below -40°C. For later Stage III fluid inclusions, the first melt was difficult to observe and hence the major cation could be either Ca and/or Na.

10.2 Secondary Fluid Inclusions

Two secondary FIFs were analyzed during the course of study. FIF TB-155-A8 was consistent in regard to final melting temperatures with a median salinity of 25.5 $CaCl_2$ equiv. wt. % (30.0 NaCl equiv. wt. %). There are two fluid inclusions in FIF TB-112-1-A11 with an estimated salinity of 2.3 $CaCl_2$ equiv. wt. % (1.7 NaCl equiv. wt. %) (Figure 17). It is clear that more information must be gathered on secondary fluid inclusions as the current picture is incomplete. The lack of data for secondary FIFs means that the

potential impact of post emplacement modification of primary and pseudosecondary FIFs by secondary fluids is poorly understood.

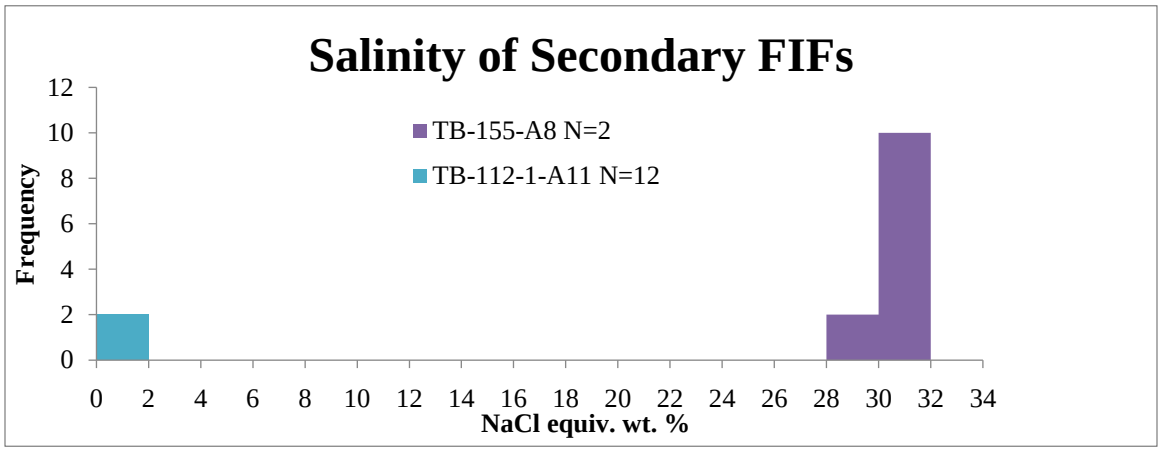

Figure 17. Salinity of Secondary FIFs. Only 2 secondary FIFs were documented for this study, TB-155-A8 and TB-112-1-A11. Salinity is expressed as NaCl equiv. wt. %.

11 Open Space Filling Calcite

One sample of calcite that was anhedral and completely filled an open space was studied using the approach and methods described previously. The calcite had an area dense with fluid inclusions with obvious lamellar twinning planes and an area of much clearer calcite that did not possess obvious lamellar twinning planes. These textures were identical to those of the calcite crystals described above. Thus, on the basis of the texture of this calcite as compared to the calcite crystals it was separated into Stage I and Stage II calcite. Under CL Stage II calcite in this sample was zoned with fluid inclusions occurring along growth zones. These fluid inclusions were classified as primary in origin based on petrographic analysis. No such zonation was visible in CL for the Stage I calcite which is similar to the calcite crystals.

No FIFs were found in Stage I calcite and one primary FIF was found within the Stage II calcite. The inconsistent homogenization temperatures of the one FIF ranged from 44.0°C to 78.0°C indicating that they do not represent primary, unmodified inclusions. Upon freezing, all inclusions of this FIF had a single solid phase with final melting temperatures at -33.0°C except for one inclusion, at -39.0°C (Figure 18). This range in homogenization and final melting temperatures is similar to Stage II primary fluid inclusions found in the vug-filling crystal samples (Figure 10 and Figure 14).

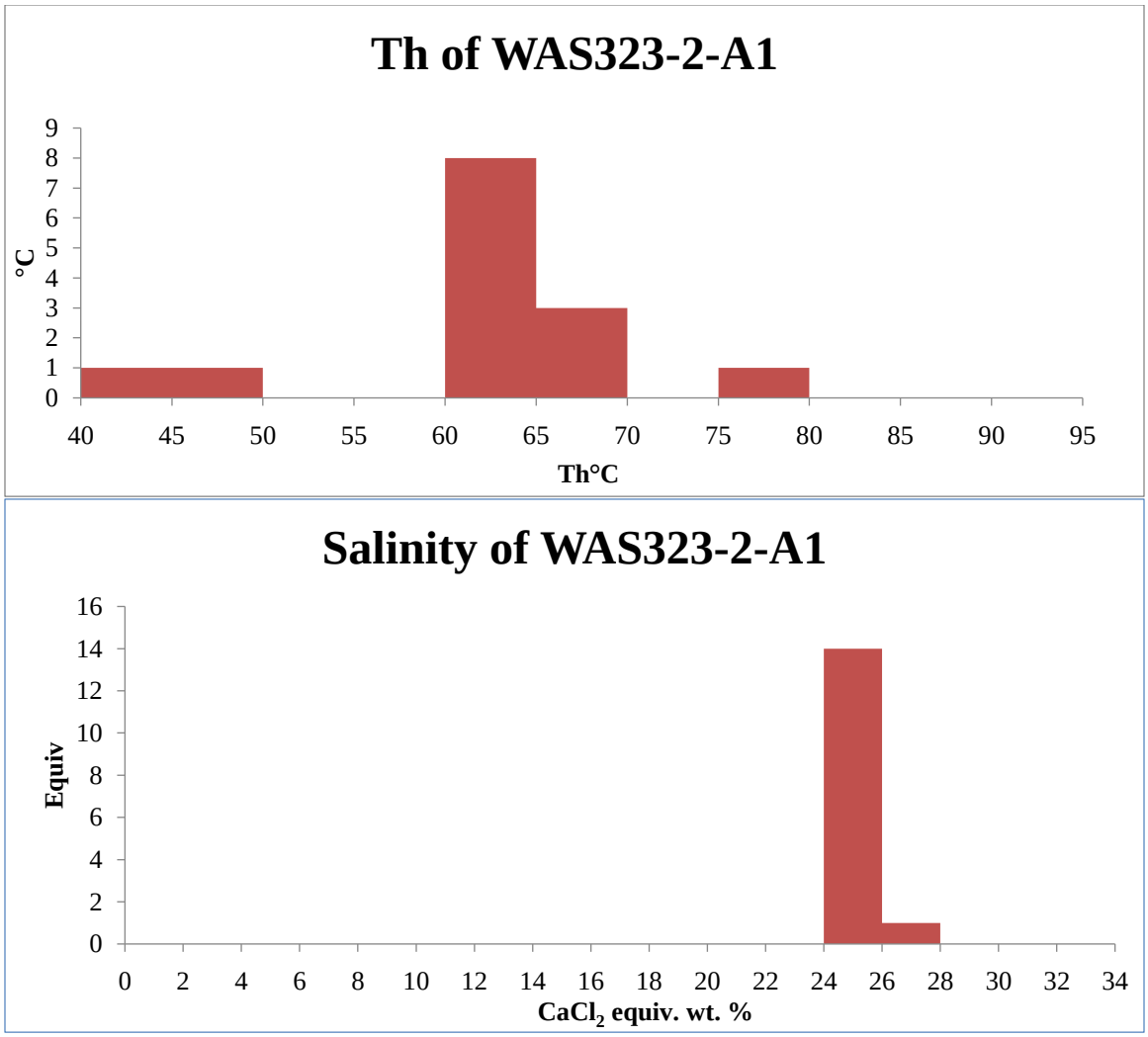

Figure 18. Homogenization and final melting temperatures of Stage II primary FIF in WAS323-2-A1. Salinity is expressed as $CaCl_2$ although there is also likely NaCl in the fluids, NaCl equivalent salinity is about 18% higher than when salinity is expressed as $CaCl_2$.Discussion

12 Discussion

12.1 Comparisons to Previous Studies

Livnat (1983) and Püschner (2001) reported homogenization temperatures of 44°C to 206°C for calcite hosted fluid inclusions. The results of this study are similar to these earlier findings in that homogenization temperatures showed a wide range.

Livnat (1983) reported that homogenization temperatures were affected by post emplacement modification. The lack of consistent homogenization temperatures for FIFs studied here indicates post emplacement modification of the fluid inclusions, and, therefore, do not likely represent the original entrapment temperature. In addition, the usefulness of homogenization temperatures is also limited by the need to apply a significant pressure correction. The likely temperature of precipitation based on mineral assemblage can be used in combination with the homogenization temperature to estimate the pressure of entrapment. Using a median homogenization temperature results in a reasonable pressure indicating that regardless of post emplacement modification the homogenization temperatures are generally representative of the conditions of formation.

Püschner (2001) and Roedder (1963) reported freezing point depressions (final melting temperatures) of -0.1°C to -45.0°C. The results of this study are consistent with these previous results having a range of 0.0°C to -54.0°C (Figure 19). Both previous reports and this report document a high variability in salinity. Some inclusions reported here did not freeze indicative of yet higher salinity. The previous reports did not note low temperature phase changes or did not provide detailed descriptions.

Prior to this study, only Roedder (1963) provided a detailed description of low temperature microthermometry. He observed a first melting temperature around -50°C and a final melting temperature of -32.5±1°C and, consequently, concluded that the brine must have contained salts other than NaCl in considerable amounts, most likely $CaCl_2$. This is consistent with the observations of this report indicating Ca-rich fluids.

Livnat (1983) determined the composition of fluid inclusions by bulk crushing tests of 9 samples of quartz, calcite, barite, and chalcocite. The leachate of these crushed samples had high Ca:Na ratios. However, these bulk leachate tests represent a composite of all generations of fluid inclusions as well as being subject to contamination, which both contribute to the uncertainty in identifying the true composition of the ore-forming fluids.

With regards to salinity and fluid composition, the current study did find similar results to the previous studies. The current report agrees with earlier assessments that Ca ions were the dominant ions in solution (at least with regard to the high salinity fluid inclusions) and that fluid inclusions could show a large range in salinity.

The high variability in the salinity of the hydrothermal fluids is unlikely to be due to post-emplacement modification since many FIFs showed good consistency with regards to final melting temperatures. On the basis of light stable isotopes, Bodden (2019) proposed that the precipitation of native copper and associated minerals involved the mixing of deep derived hydrothermal/metamorphogenic fluids and relatively shallow resident meteoric waters. The high variability of salinity can be explained by entrapment of variable proportions of high salinity hydrothermal/metamorphogenic fluids with low salinity meteoric waters.

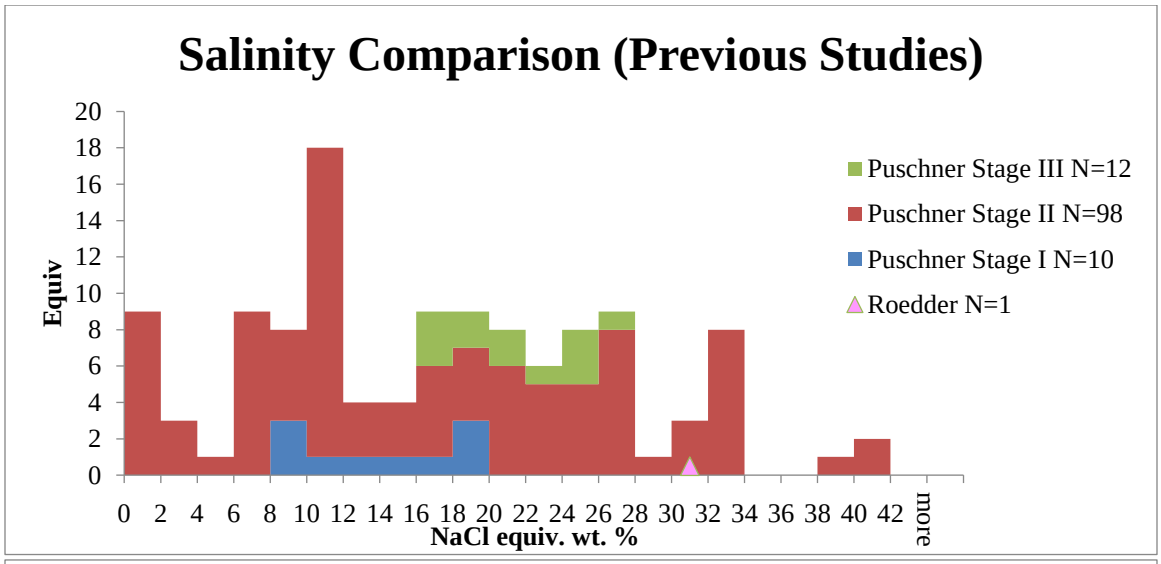

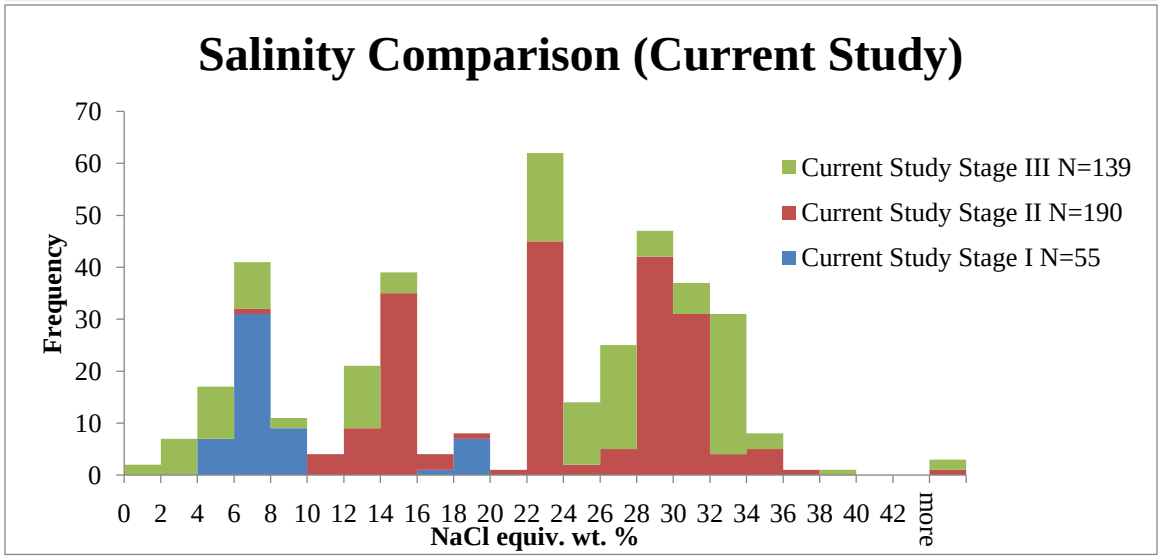

Figure 19. Comparison of salinities from other fluid inclusion studies. The results of Püschner (2001) are displayed for calcite samples dived into 3 stages. Only one data point was available for Roedder (1963). The data from the current study is displayed below and are potentially biased because fluid inclusions from an FIF were plotted as individual distinct measurements of points in time whereas the FIF actually represents a short (single) interval of time. Results are given in NaCl equivalents as previous studies originally used this to calculate salinities.

12.2 Limitations of this Study and Recommendations for Future Fluid Inclusion Work

Both post-emplacement modification and pressure corrections limited the usefulness of fluid inclusion homogenization temperatures in this work. Pressure corrections are not needed for fluid salinity estimates obtained from melting temperatures. The potential effect of post emplacement modification on salinity is currently unknown. Additional study of the salinity of secondary fluid inclusions is needed to assist in the understanding of post fluid inclusion entrapment modification of salinity. The study of fluid salinity in these inclusions is likely to be more useful than homogenization temperatures and could be the focus of a future study.

This study was limited by the unknown location of the vug-filling calcite crystals which could shed doubt on their representativeness. However, after comparing the results of this study with those of Püschner (2001), the results of this current report appear to be representative.

Although the main focus of this study was to further our understanding of the native copper fluids, more work could be done precipitation that predated and postdated the native copper event. Suitable samples for this purpose have even been identified through the course of this study, but as they were only likely to yield data from a time other than the native copper event they were dismissed from study.

Acquisition of additional chemical data from the fluid inclusions could provide valuable information on the compositional evolution of the fluids before, during, and after the main stage of copper mineralization. Expanding the study of fluid inclusions beyond the Quincy Mine could also provide useful information on the regional differences in fluid compositions.

13 Conclusions

The conclusions of this report are:

1. Three stages of calcite were found, which were consistent with those described by Püschner (2001). Stage I and II were formed during the main-stage hydrothermal event that also for the native copper mineralization. Stage III was formed by a later post native copper hydrothermal event.
2. Under CL Stage I had almost no growth zones. Stage II had a jigsaw pattern indicative of rapid growth. Stage III had regular growth zoning, indicating slower growth than Stage II.
3. Chalcocite was found exclusively within Stage III calcite with a mossy texture chalcocite found near the Stage II boundary and a later arborescent texture chalcocite found near the end of all crystal growth.
4. Only pseudosecondary FIFs could be identified within the Stage I calcite. Decrepitation structures were also identified within this stage and suggest overheating occurred during this stage.
5. Primary fluid inclusions as well as pseudosecondary fluid inclusions were identified in Stage II and Stage III calcite.
6. The variability of homogenization temperatures of the fluid inclusions within given FIFs found in this report indicate that post entrapment changes have occurred.
7. Homogenization temperatures for FIFs across all stages were not consistent, however, the median homogenization temperatures are believed to approximate the original trapping temperatures uncorrected for pressure.
8. Final melting temperatures could show good consistency within certain FIFs. Stage I ranged from 5.9-18.4 $CaCl_2$ equiv. wt. % (5.0-19.5 NaCl equiv. wt. %). Stage II ranged from 8.9-30.7 $CaCl_2$ equiv. wt. % (7.9-54.9 NaCl equiv. wt. %). Stage III ranged from 0.0-30.5 $CaCl_2$ equiv. wt. % (0.0-49.7 NaCl equiv. wt. %). with earlier FIFs associated with mossy texture chalcocite having a higher salinity than those associated with arborescent texture chalcocite. It is not certain if the high variability of salinity is primary or a result of post-emplacement modification.
9. The high salinity fluids were likely Ca rich. It is not known if the lower salinity fluids were Ca or Na rich.
10. Open space filling calcite showed very similar petrography, homogenization temperatures, and salinities to the vug-filling calcite crystals.
11. The high variability in salinity is best explained by variable fluid mixing of high salinity and low salinity fluids.

14 Reference List

Bodden, T., 2019, Spatial and Temporal Distribution of Hydrothermal Minerals and Sources of Hydrothermal Fluids Inferred from Light Stable Isotopes, Keweenaw Peninsula Native Copper District, Michigan.

Bodnar, R., 1993, Revised equation and table for determining the freezing point depression of H2O-NaCl solutions: Geochimica et Cosmochimica acta, v. 57, no. 3, p. 683-684.

Bornhorst, T. J., and Lankton, L. D., 2012, Copper mining: A billion years of geologic and human history.

Bornhorst, T. J., and Mathur, R., 2017, Copper Isotope Constraints on the Genesis of the Keweenaw Peninsula Native Copper District, Michigan, USA: Minerals, v. 7, no. 10, p. 185.

Bornhorst, T. J., and McDowell, S. D., Michigan Tech Earth Science Laboratory and Experimental Mine Connecting With The Quincy Native Copper Mine, Michigan, *in* Proceedings Keweenawan copper deposits of western upper Michigan: guidebook prepared for Society of Economic Geologists field conference, 20-23 1992, Volume 13, Dept. of Earth Resources, Colorado State University, p. 99.

Bornhorst, T. J., Paces, J. B., Grant, N. K., Obradovich, J. D., and Huber, N. K., 1988, Age of native copper mineralization, Keweenaw Peninsula, Michigan: Economic Geology, v. 83, no. 3, p. 619-625.

Bornhorst, T. J., and Rose, W. I., 1994, Self-guided geological field trip to the Keweenaw Peninsula, Michigan, The Institute on Lake Superior Geology.

Bumgarner, E. L., 1980, The Geology of the Portage Lake Volcanics in the MTU Mining Laboratory Hancock, Michigan: Michigan Technological University.

Butler, B. S., and Burbank, W. S., 1929, The copper deposits of Michigan, US Government Printing Office, v. 144.

Cannon, W., Peterman, Z., and Sims, P., 1993, Crustal-scale thrusting and origin of the Montreal River monocline-A 35-km-thick cross section of the midcontinent rift in northern Michigan and Wisconsin: Tectonics, v. 12, no. 3, p. 728-744.

Cannon, W. F., 1994, Closing of the Midcontinent rift-A far—field effect of Grenvillian compression: Geology, v. 22, no. 2, p. 155-158.

Davis, D., and Paces, J., 1990, Time resolution of geologic events on the Keweenaw Peninsula and implications for development of the Midcontinent Rift system: Earth and Planetary Science Letters, v. 97, no. 1-2, p. 54-64.

Davis, D. W., Lowenstein, T. K., and Spencer, R. J., 1990, Melting behavior of fluid inclusions in laboratory-grown halite crystals in the systems NaCl□ H2O, NaCl□ KCl□ H2O, NaCl□ MgCl2□ H2O, and NaCl□ CaCl2□ H2O: Geochimica et Cosmochimica Acta, v. 54, no. 3, p. 591-601.

Goldstein, R. H., and Reynolds, T. J., 1994, Systematics of fluid inclusions in diagenetic minerals, Tulsa, Okla., SEPM, SEPM short course, v. 31, xii, 199 p. p.:

Jolly, W. T., and Smith, R. E., 1972, Degradation and metamorphic differentiation of the Keweenawan tholeiitic lavas of northern Michigan, USA: Journal of Petrology, v. 13, no. 2, p. 273-309.

Livnat, A., 1983, Metamorphism and copper mineralization of the Portage Lake lava series, northern Michigan: Unpub: Ph. D. dissertation, University of Michigan.

Moncada, D., Mutchler, S., Nieto, A., Reynolds, T., Rimstidt, J., and Bodnar, R., 2012, Mineral textures and fluid inclusion petrography of the epithermal Ag–Au deposits at Guanajuato, Mexico: Application to exploration: Journal of Geochemical Exploration, v. 114, p. 20-35.

Oakes, C. S., Bodnar, R. J., and Simonson, J. M., 1990, The system NaCl□ CaCl2□ H2O: I. The ice liquidus at 1 atm total pressure: Geochimica et Cosmochimica Acta, v. 54, no. 3, p. 603-610.

Paces, J. B., 1988, Magmatic processes, evolution and mantle source characteristics contributing to the petrogenesis of Midcontinent rift basalts: Portage Lake Volcanics, Keweenaw Peninsula.

Palache, C., 1898, The crystallization of the calcite from the copper mines of Lake Superior, Geological Survey of Michigan.

Potter, R. W. I., 1977, Pressure corrections for fluid-inclusion homogenization temperatures based on the volumetric properties of the system NaCl-H 2 O: Journal of Research of the US Geological Survey, v. 5, no. 5, p. 603-607.

Price, K. L., and McDowell, S. D., 1993, Illite/smectite geothermometry of the Proterozoic Oronto Group, midcontinent rift system: Clays and Clay Minerals, v. 41, no. 2, p. 134-147.

Püschner, U. R., 2001, Very low-grade metamorphism in the Portage Lake Volcanics on the Keweenaw Peninsula, Michigan, USA: University_of_Basel.

Richards, J., and Spooner, E., 1986, Native copper deposition by mixing of high temperature, high salinity fluids of possible magmatic association, with cool dilute groundwaters, Keweenaw Peninsula, Michigan labs. I: Geol. Soc: America Abstracts with Program, v. 18, p. 730.

Roedder, E., 1963, Studies of fluid inclusions;[Part] 2, Freezing data and their interpretation: Economic Geology, v. 58, no. 2, p. 167-211.

-, 1984, Fluid inclusions : an introduction to studies of all types of fluid inclusions, gas, liquid, or melt, trapped in materials from earth and space, and their application to the understanding of geologic processes, Washington, D.C., Mineralogical Society of America, Reviews in mineralogy, v. 12, vi, 644 p. p.:

Samson, I., Anderson, A., and Marshall, D. D., 2003, Fluid inclusions : analysis and interpretation, Ottawa, Ont., Canada, Mineralogical Association of Canada, Short course series, v. 32, vi, 374 p., 371 p. of plates p.:

Schleiss, W. A., 1986, A Study of Vein Mineralization and Wall Rock Alteration at the Delaware Mine, Keweenaw County, Michigan: Michigan Technological University.

Spencer, R. J., Møller, N., and Weare, J. H., 1990, The prediction of mineral solubilities in natural waters: A chemical equilibrium model for the Na□ K□ Ca□ Mg□ Cl□

SO4□ H2O system at temperatures below 25°C: Geochimica et Cosmochimica Acta, v. 54, no. 3, p. 575-590.

Stoiber, R. E., and Davidson, E. S., 1959, Amygdule mineral zoning in the Portage Lake Lava series, Michigan copper district; Part 1: Economic Geology, v. 54, no. 7, p. 1250-1277.

Van den Kerkhof, A. M., and Hein, U. F., 2001, Fluid inclusion petrography: Lithos, v. 55, no. 1-4, p. 27-47.

Weege, R., and Pollack, J., Recent developments in the native-copper district of Michigan, *in* Proceedings Society of Economic Geologists Guidebook for Field Conference, Michigan Copper District1971, p. 18-43.

Wilkinson, J., 2001, Fluid inclusions in hydrothermal ore deposits: Lithos, v. 55, no. 1-4, p. 229-272.

15 Appendix

Table 1. Fluid Inclusion Microthermometry Data

FIF	FIID	Origin	Size (μm)	Phases	Solids	Shape	Th (°C)	Tm (°C)	Ice	Stage	NaCl wt%	$CaCl_2$ wt%	Note
TB-112-1-?	1	P	22.91	-	none	irregular	9999	-32.0	1	2	30.0	25.5	identified post heating
TB-112-1-?	2	P	45.64	LV	none	very irregular	67.0	-24.0	1	2	21.5	22.5	
TB-112-1-A1	3	Ps	4.74	LV	none	faceted	97.0	-5.0	1	1	7.9	8.9	
TB-112-1-A1	4	Ps	5.00	LV	none	faceted	128.0	-5.0	1	1	7.9	8.9	
TB-112-1-A1	5	Ps	7.29	LV	none	faceted	123.0	9999	-	1	9999	9999	hard to see ice
TB-112-1-A1	6	Ps	7.43	LV	none	faceted	92.0	-5.0	1	1	7.9	8.9	
TB-112-1-A1	7	Ps	7.83	LV	none	faceted	118.0	-5.0	1	1	7.9	8.9	
TB-112-1-A1	8	Ps	9.58	LV	none	faceted	129.0	-14.0	1	1	17.8	17.1	
TB-112-1-A1	9	Ps	10.36	LV	none	faceted	125.0	-5.0	1	1	7.9	8.9	
TB-112-1-A1	10	Ps	10.45	LV	none	faceted	9999	-5.0	1	1	7.9	8.9	
TB-112-1-A1	11	Ps	10.64	LV	none	faceted	137.0	-5.0	1	1	7.9	8.9	
TB-112-1-A1	12	Ps	15.53	LV	none	faceted	120.0	-5.0	1	1	7.9	8.9	
TB-112-1-A10	13	P	11.58	LV	none	irregular	92.0	-31.0	1	3	29.3	25.2	
TB-112-1-A10	14	P	18.35	LV	none	irregular elongate	83.0	-32.0	1	3	30.0	25.5	
TB-112-1-A10	15	P	19.07	LV	none	irregular	9999	-38.0	1	3	34.4	27.3	
TB-112-1-A10	16	P	20.24	LV	none	very irregular	9999	-37.0	1	3	33.6	27.1	
TB-112-1-A10	17	P	24.13	LV	none	irregular	67.0	-35.0	1	3	32.0	26.5	
TB-112-1-A10	18	P	33.04	L	none	irregular	<50	9999	1	3	9999	9999	
TB-112-1-A10	19	P	37.37	LV	none	very irregular	83.0	-32.0	1	3	30.0	25.5	
TB-112-1-A10	20	P	48.51	LV	none	irregular	84.0	9999	1	3	9999	9999	
TB-112-1-A10	21	P	51.24	LV	none	very irregular	103.0	9999	1	3	9999	9999	
TB-112-1-A10	22	P	72.48	LV	none	irregular	60.0	9999	1	3	9999	9999	
TB-112-1-A11	23	S	6.10	-	none	elongate	9999	-1.0	1	?	1.7	2.3	identified post heating
TB-112-1-A11	24	S	8.39	-	none	elongate	9999	-1.0	1	?	1.7	2.3	identified post heating
TB-112-1-A12	25	Ps	6.26	-	none	faceted	9999	-5.0	1	3	7.9	8.9	identified post heating
TB-112-1-A12	26	Ps	6.55	-	none	faceted	9999	-5.0	1	3	7.9	8.9	identified post heating
TB-112-1-A12	27	Ps	7.23	-	none	elongate	9999	-5.0	1	3	7.9	8.9	identified post heating
TB-112-1-A12	28	Ps	7.39	-	none	faceted?	9999	-5.0	1	3	7.9	8.9	identified post heating
TB-112-1-A12	29	Ps	7.80	-	none	faceted	9999	-6.0	1	3	9.2	10.1	identified post heating
TB-112-1-A12	30	Ps	7.96	-	none	faceted	9999	-5.0	1	3	7.9	8.9	identified post heating
TB-112-1-A13	31	Ps	8.17	-	none	elongate	9999	-10.0	1	3	13.9	14.2	identified post heating
TB-112-1-A13	32	Ps	8.21	-	none	faceted elongate	9999	-10.0	1	3	13.9	14.2	identified post heating
TB-112-1-A13	33	Ps	8.36	-	none	faceted?	9999	-10.0	1	3	13.9	14.2	identified post heating
TB-112-1-A13	34	Ps	9.17	-	none	spherical	9999	-9.0	1	3	12.8	13.3	identified post heating
TB-112-1-A13	35	Ps	10.55	-	none	elongate	9999	-10.0	1	3	13.9	14.2	identified post heating
TB-112-1-A13	36	Ps	11.00	-	none	elongate	9999	-10.0	1	3	13.9	14.2	identified post heating
TB-112-1-A13	37	Ps	11.57	-	none	irregular faceted	9999	-11.0	1	3	15.0	15.0	identified post heating
TB-112-1-A13	38	Ps	12.93	-	none	elongate irregular	9999	-11.0	1	3	15.0	15.0	identified post heating
TB-112-1-A14	39	Ps	6.30	-	none	spherical	9999	-25.0	1	3	25.6	22.9	identified post heating
TB-112-1-A14	40	Ps	7.02	-	none	faceted	9999	-25.0	1	3	25.6	22.9	identified post heating
TB-112-1-A14	41	Ps	7.50	-	none	faceted	9999	-26.0	1	3	26.2	23.3	identified post heating
TB-112-1-A14	42	Ps	7.70	-	none	faceted	9999	-25.0	1	3	25.6	22.9	identified post heating
TB-112-1-A14	43	Ps	8.49	-	none	elongate faceted?	9999	-24.0	1	3	25.0	22.5	identified post heating
TB-112-1-A14	44	Ps	9.16	-	none	elongate	9999	-25.0	1	3	25.6	22.9	identified post heating
TB-112-1-A15	45	Ps	6.25	-	none	faceted	9999	-26.0	1	3	26.2	23.3	identified post heating
TB-112-1-A15	46	Ps	6.67	-	none	faceted	9999	-26.0	1	3	26.2	23.3	identified post heating
TB-112-1-A15	47	Ps	7.29	-	none	faceted?	9999	-27.0	1	3	26.8	23.7	identified post heating
TB-112-1-A15	48	Ps	7.41	-	none	elongate	9999	-27.0	1	3	26.8	23.7	identified post heating
TB-112-1-A15	49	Ps	7.48	-	none	faceted	9999	-27.0	1	3	26.8	23.7	identified post heating
TB-112-1-A15	50	Ps	9.36	-	none	irregular	9999	-26.0	1	3	26.2	23.3	identified post heating
TB-112-1-A15	51	Ps	9.49	-	none	spherical	9999	-26.0	1	3	26.2	23.3	identified post heating
TB-112-1-A15	52	Ps	14.26	-	none	irregular elongate	9999	-27.0	1	3	26.8	23.7	identified post heating
TB-112-1-A16	53	P	7.42	-	none	irregular	9999	-31.0	1	2	29.3	25.2	identified post heating
TB-112-1-A16	54	P	11.90	-	none	very irregular	9999	-28.0	1	2	27.4	24.1	identified post heating

Table 1 continued. Fluid Inclusion Microthermometry Data

FIF	FIID	Origin	Size (μm)	Phases	Solids	Shape	Th (°C)	Tm (°C)	Ice	Stage	NaCl wt%	$CaCl_2$ wt%	Note
TB-112-1-A16	55	P	12.87	-	none	irregular	9999	-24.0	1	2	25.0	22.5	identified post heating
TB-112-1-A18	56	Ps	5.05	LV	none	faceted	111.0	-12.0	1	2	16.0	15.7	
TB-112-1-A18	57	Ps	5.30	LV	none	faceted	9999	-13.0	1	2	16.9	16.4	hard to see bubble
TB-112-1-A18	58	Ps	6.83	LV	none	faceted	84.0	-11.0	1	2	15.0	15.0	
TB-112-1-A18	59	Ps	7.29	LV	none	faceted irregular	85.0	-16.0	1	2	19.4	18.4	
TB-112-1-A18	60	Ps	7.49	LV	none	faceted	99.0	-11.0	1	2	15.0	15.0	
TB-112-1-A18	61	Ps	7.93	LV	none	faceted	107.0	9999	1	2	9999	9999	
TB-112-1-A18	62	Ps	7.93	LV	none	faceted	109.0	-12.0	1	2	16.0	15.7	
TB-112-1-A18	63	Ps	8.08	LV	none	faceted	131.0	-12.0	1	2	16.0	15.7	
TB-112-1-A18	64	Ps	8.32	LV	none	faceted	102.0	-12.0	1	2	16.0	15.7	
TB-112-1-A18	65	Ps	12.25	LV	none	faceted	105.0	-12.0	1	2	16.0	15.7	
TB-112-1-A18	66	Ps	12.28	LV	none	faceted	106.0	-12.0	1	2	16.0	15.7	
TB-112-1-A18	67	Ps	19.57	LV	none	irregular	138.0	-13.0	1	2	16.9	16.4	
TB-112-1-A18	68	Ps	25.13	LV	none	irregular faceted	137.0	-12.0	1	2	16.0	15.7	
TB-112-1-A18	69	Ps	32.72	LV	none	irregular	139.0	-12.0	1	2	16.0	15.7	
TB-112-1-A2	70	Ps	3.19	LV	none	faceted	131.0	-10.0	1	2	13.9	14.2	
TB-112-1-A2	71	Ps	4.79	LV	none	faceted	76.0	-12.0	1	2	16.0	15.7	
TB-112-1-A2	72	Ps	4.79	LV	none	faceted	128.0	-11.0	1	2	15.0	15.0	
TB-112-1-A2	73	Ps	4.91	LV	none	faceted	129.0	-11.0	1	2	15.0	15.0	
TB-112-1-A2	74	Ps	4.92	LV	none	faceted	9999	-11.0	1	2	15.0	15.0	
TB-112-1-A2	75	Ps	5.82	LV	none	faceted	123.0	-12.0	1	2	16.0	15.7	
TB-112-1-A2	76	Ps	6.34	LV	none	faceted	86.0	-14.0	1	2	17.8	17.1	
TB-112-1-A2	77	Ps	6.46	LV	none	faceted	9999	-11.0	1	2	15.0	15.0	
TB-112-1-A2	78	Ps	6.80	LV	none	faceted	128.0	9999	1	2	9999	9999	
TB-112-1-A2	79	Ps	7.01	LV	none	faceted	128.0	-12.0	1	2	16.0	15.7	
TB-112-1-A2	80	Ps	7.86	LV	none	faceted	125.0	-11.0	1	2	15.0	15.0	
TB-112-1-A2	81	Ps	8.32	LV	none	faceted	125.0	-12.0	1	2	16.0	15.7	
TB-112-1-A2	82	Ps	8.39	LV	none	faceted	126.0	-11.0	1	2	15.0	15.0	
TB-112-1-A2	83	Ps	9.83	LV	none	faceted	129.0	-11.0	1	2	15.0	15.0	
TB-112-1-A2	84	Ps	10.85	LV	none	faceted	127.0	-11.0	1	2	15.0	15.0	
TB-112-1-A2	85	Ps	11.50	LV	none	faceted	122.0	-12.0	1	2	16.0	15.7	
TB-112-1-A2	86	Ps	12.42	LV	none	faceted	125.0	9999	1	2	9999	9999	
TB-112-1-A2	87	Ps	12.94	LV	none	elongate faceted	130.0	9999	1	2	9999	9999	
TB-112-1-A2	88	Ps	13.00	LV	none	faceted	115.0	9999	1	2	9999	9999	
TB-112-1-A2	89	Ps	15.62	LV	none	faceted	124.0	-12.0	1	2	16.0	15.7	
TB-112-1-A2	90	Ps	15.87	LV	none	faceted	130.0	-12.0	1	2	16.0	15.7	
TB-112-1-A2	91	Ps	16.69	LV	none	faceted	133.0	-5.0	1	2	7.9	8.9	
TB-112-1-A2	92	Ps	18.17	LV	none	faceted	119.0	-11.0	1	2	15.0	15.0	
TB-112-1-A2	93	Ps	18.41	LV	none	irregular	131.0	9999	1	2	9999	9999	
TB-112-1-A2	94	Ps	19.03	LV	none	irregular	126.0	-11.0	1	2	15.0	15.0	
TB-112-1-A2	95	Ps	19.17	LV	none	faceted	126.0	-11.0	1	2	15.0	15.0	
TB-112-1-A2	96	Ps	19.30	LV	none	faceted	129.0	9999	1	2	9999	9999	
TB-112-1-A2	97	Ps	19.99	LV	none	spherical	128.0	9999	1	2	9999	9999	
TB-112-1-A2	98	Ps	20.69	LV	none	faceted	127.0	-11.0	1	2	15.0	15.0	
TB-112-1-A2	99	Ps	21.09	LV	none	faceted	128.0	-11.0	1	2	15.0	15.0	
TB-112-1-A2	100	Ps	23.90	LV	none	irregular	152.0	-9.0	1	2	12.8	13.3	
TB-112-1-A2	101	Ps	26.15	LV	none	faceted	126.0	-12.0	1	2	16.0	15.7	
TB-112-1-A2	102	Ps	30.77	LV	none	irregular	120.0	-10.0	1	2	13.9	14.2	
TB-112-1-A2	103	Ps	33.03	LV	none	irregular	129.0	9999	1	2	9999	9999	
TB-112-1-A2	104	Ps	40.67	LV	none	irregular elongate	128.0	-9.0	1	2	12.8	13.3	
TB-112-1-A2	105	Ps	42.35	LV	none	faceted	132.0	9999	1	2	9999	9999	
TB-112-1-A2	106	Ps	42.71	LV	none	irregular	120.0	-11.0	1	2	15.0	15.0	
TB-112-1-A2	107	Ps	60.49	LV	none	irregular	166.0	-7.0	1	2	10.5	11.3	
TB-112-1-A20	108	P	14.96	L	none	irregular elongate	<50	9999	1	2	9999	9999	

Table 1 continued. Fluid Inclusion Microthermometry Data

FIF	FIID	Origin	Size (μm)	Phases	Solids	Shape	Th (°C)	Tm (°C)	Ice	Stage	NaCl wt%	$CaCl_2$ wt%	Note
TB-112-1-A20	109	P	23.08	LV	none	irregular elongate	60.0	-33.0	1	2	30.6	25.9	
TB-112-1-A22	110	P	39.25	LV	none	irregular	67.0	-33.0	1	2	30.6	25.9	
TB-112-1-A22	111	P	67.09	LV	none	irregular	70.0	-32.0	1	2	30.0	25.5	
TB-112-1-A23	112	P	9.12	LV	none	irregular	60.0	-25.0	1	2	25.6	22.9	
TB-112-1-A23	113	P	15.69	LV	none	irregular	76.0	-28.0	1	2	27.4	24.1	
TB-112-1-A3	114	Ps	3.41	LV	none	faceted	102.0	9999	-	1	9999	9999	hard to see ice
TB-112-1-A3	115	Ps	4.10	LV	none	faceted	104.0	9999	-	1	9999	9999	hard to see ice
TB-112-1-A3	116	Ps	4.66	-	none	faceted	9999	-3.0	1	1	5.0	5.9	identified post heating
TB-112-1-A3	117	Ps	4.98	-	none	faceted	9999	-3.0	1	1	5.0	5.9	identified post heating
TB-112-1-A3	118	Ps	5.25	-	none	faceted	9999	-3.0	1	1	5.0	5.9	identified post heating
TB-112-1-A3	119	Ps	5.33	LV	none	faceted	107.0	9999	-	1	9999	9999	hard to see ice
TB-112-1-A3	120	Ps	8.01	-	none	spherical elongate	9999	-3.0	1	1	5.0	5.9	identified post heating
TB-112-1-A3	121	Ps	8.49	LV	none	spherical	117.0	9999	-	1	9999	9999	hard to see ice
TB-112-1-A3	122	Ps	10.03	-	none	faceted elongate	9999	-3.0	1	1	5.0	5.9	identified post heating
TB-112-1-A3	123	Ps	11.89	-	none	faceted irregular	9999	-3.0	1	1	5.0	5.9	identified post heating
TB-112-1-A3	124	Ps	15.69	-	none	faceted elongate	9999	-3.0	1	1	5.0	5.9	identified post heating
TB-112-1-A4	125	P	6.97	LV	none	irregular	57.0	-31.0	1	2	29.3	25.2	
TB-112-1-A4	126	P	9.05	LV	none	irregular	54.0	-31.0	1	2	29.3	25.2	
TB-112-1-A4	127	P	15.80	LV	none	irregular	77.0	-27.0	1	2	26.8	23.7	
TB-112-1-A5	128	Ps	6.35	LV	none	spherical	57.0	-36.0	1	3	32.8	26.8	
TB-112-1-A5	129	Ps	6.40	LV	none	spherical	61.0	-36.0	1	3	32.8	26.8	
TB-112-1-A5	130	Ps	7.42	LV	none	spherical	70.0	-36.0	1	3	32.8	26.8	
TB-112-1-A5	131	Ps	7.42	LV	none	spherical	73.0	-36.0	1	3	32.8	26.8	
TB-112-1-A5	132	Ps	8.00	LV	none	faceted	63.0	-36.0	1	3	32.8	26.8	
TB-112-1-A5	133	Ps	8.42	LV	none	spherical	66.0	-36.0	1	3	32.8	26.8	
TB-112-1-A5	134	Ps	9.44	LV	none	spherical	59.0	-36.0	1	3	32.8	26.8	
TB-112-1-A5	135	Ps	10.08	LV	none	spherical	9999	-34.0	1	3	31.3	26.2	
TB-112-1-A5	136	Ps	11.36	LV	none	spherical	59.0	-36.0	1	3	32.8	26.8	
TB-112-1-A5	137	Ps	11.99	LV	none	spherical	69.0	-36.0	1	3	32.8	26.8	
TB-112-1-A5	138	Ps	12.11	LV	none	irregular	61.0	-36.0	1	3	32.8	26.8	
TB-112-1-A5	139	Ps	12.94	LV	none	faceted	57.0	-36.0	1	3	32.8	26.8	
TB-112-1-A5	140	Ps	14.24	LV	none	faceted	52.0	-35.0	1	3	32.0	26.5	
TB-112-1-A5	141	Ps	14.63	LV	none	faceted	66.0	-36.0	1	3	32.8	26.8	
TB-112-1-A5	142	Ps	15.52	LV	none	faceted	63.0	-36.0	1	3	32.8	26.8	
TB-112-1-A6	143	Ps	5.84	-	none	faceted	9999	-11.0	1	3	15.0	15.0	identified post heating
TB-112-1-A6	144	Ps	7.11	-	none	faceted	9999	-10.0	1	3	13.9	14.2	identified post heating
TB-112-1-A6	145	Ps	7.92	L	none	spherical	<50	-6.0	1	3	9.2	10.1	
TB-112-1-A6	146	Ps	8.89	L	none	spherical	<50	9999	-	3	9999	9999	hard to see ice
TB-112-1-A6	147	Ps	9.84	-	none	faceted	9999	-10.0	1	3	13.9	14.2	identified post heating
TB-112-1-A6	148	Ps	19.96	L	none	elongate	<50	-10.0	1	3	13.9	14.2	
TB-112-1-A6	149	Ps	20.04	L	none	elongate	<50	-10.0	1	3	13.9	14.2	
TB-112-1-A6	150	Ps	44.76	L	none	irregular	<50	-10.0	1	3	13.9	14.2	
TB-112-1-A6	151	Ps	47.81	L	none	irregular elongate	<50	-11.0	1	3	15.0	15.0	
TB-112-1-A6	152	Ps	53.91	L	none	very irregular	<50	-10.0	1	3	13.9	14.2	
TB-112-1-A6	153	Ps	70.46	L	none	irregular elongate	<50	9999	1	3	9999	9999	
TB-112-1-A8	154	P	5.89	LV	none	irregular	9999	-26.0	1	2	26.2	23.3	
TB-112-1-A8	155	P	15.39	LV	none	very irregular	73.0	-30.0	1	2	28.7	24.8	
TB-112-1-A8	156	P	15.55	LV	none	irregular	76.0	-29.0	1	2	28.0	24.5	
TB-112-1-A8	157	P	19.80	LV	none	irregular	9999	-26.0	1	2	26.2	23.3	
TB-112-1-A8	158	P	28.29	LV	none	very irregular	79.0	-29.0	1	2	28.0	24.5	
TB-155-?	159	P	3.61	L	copper	spherical	<50	-33.0	1	2	30.6	25.9	
TB-155-?	160	P	4.54	LV	copper	spherical	56.0	9999	-	2	9999	9999	hard to see ice
TB-155-?	161	P	4.64	LV	copper	irregular	71.0	9999	-	2	9999	9999	hard to see ice
TB-155-?	162	P	5.47	LV	copper	spherical	68.0	-34.0	1	2	31.3	26.2	

Table 1 continued. Fluid Inclusion Microthermometry Data

FIF	FIID	Origin	Size (μm)	Phases	Solids	Shape	Th (°C)	Tm (°C)	Ice	Stage	NaCl wt%	$CaCl_2$ wt%	Note
TB-155-?	163	P	5.80	LV	copper	spherical	69.0	-33.0	1	2	30.6	25.9	
TB-155-?	164	P	5.86	LV	copper	irregular	73.0	9999	-	2	9999	9999	hard to see ice
TB-155-?	165	P	6.22	LV	copper	irregular	62.0	-35.0	1	2	32.0	26.5	
TB-155-?	166	P	6.68	LV	copper	irregular	71.0	-11.0	2	2	>23.2	>23.2	
TB-155-?	167	P	6.68	LV	copper	irregular	83.0	-31.0	1	2	29.3	25.2	
TB-155-?	168	P	6.99	L	copper	spherical	<50	-39.0	1	2	35.2	27.6	
TB-155-?	169	P	7.29	LV	copper	spherical	63.0	-33.0	1	2	30.6	25.9	
TB-155-?	170	P	7.84	LV	copper	elongate	65.0	-39.0	1	2	35.2	27.6	
TB-155-?	171	P	7.88	LV	copper	elongate	65.0	9999	-	2	9999	9999	hard to see ice
TB-155-?	172	P	8.31	LV	copper	spherical	65.0	-34.0	1	2	31.3	26.2	
TB-155-?	173	P	8.44	LV	copper	elongate	71.0	-37.0	1	2	33.6	27.1	
TB-155-?	174	P	9.33	LV	copper	spherical	70.0	-34.0	1	2	31.3	26.2	
TB-155-?	175	P	10.43	LV	copper	irregular	80.0	-35.0	1	2	32.0	26.5	
TB-155-?	176	P	10.71	LV	copper	spherical	64.0	-31.0	1	2	29.3	25.2	copper broke off
TB-155-?	177	P	11.21	LV	copper	irregular	69.0	9999	-	2	9999	9999	hard to see ice
TB-155-?	178	P	11.60	LV	copper	irregular	69.0	-29.0	2	2	>23.2	>23.2	
TB-155-?	179	P	11.66	LV	copper	faceted	65.0	-39.0	1	2	35.2	27.6	
TB-155-?	180	P	12.94	LV	copper	elongate	77.0	-33.0	1	2	30.6	25.9	
TB-155-?	181	P	13.15	LV	copper	spherical	76.0	-33.0	1	2	30.6	25.9	
TB-155-?	182	P	13.79	LV	copper	spherical	65.0	-12.0	2	2	>23.2	>23.2	
TB-155-?	183	P	14.22	LV	copper	elongate	63.0	-35.0	1	2	32.0	26.5	
TB-155-?	184	P	14.45	LV	copper	spherical	68.0	-18.0	2	2	>23.2	>23.2	
TB-155-?	185	P	14.46	LV	copper	irregular	63.0	9999	-	2	9999	9999	hard to see ice
TB-155-?	186	P	14.78	LV	copper	spherical	68.0	-13.0	2	2	>23.2	>23.2	
TB-155-?	187	P	15.04	LV	copper	irregular	67.0	9999	-	2	9999	9999	hard to see ice
TB-155-?	188	P	16.96	LV	copper	irregular	64.0	9999	1	2	9999	9999	
TB-155-?	189	P	18.18	LV	copper	irregular	67.0	-15.0	2	2	>23.2	>23.2	
TB-155-?	190	P	20.16	LV	copper	very irregular	87.0	-18.0	2	2	>23.2	>23.2	
TB-155-?	191	P	20.54	LV	copper	faceted	84.0	9999	1	2	9999	9999	
TB-155-?	192	P	24.71	LV	copper	irregular	110.0	-32.0	1	2	30.0	25.5	
TB-155-?	193	P	25.42	LV	copper	irregular	71.0	-11.0	2	2	>23.2	>23.2	
TB-155-?	194	P	26.00	LV	copper	irregular	76.0	-13.0	2	2	>23.2	>23.2	
TB-155-?	195	P	27.87	LV	copper	irregular	71.0	WNF	-	2	>30.5	>30.5	would not freeze
TB-155-?	196	P	30.04	LV	copper	very irregular	79.0	9999	1	2	9999	9999	
TB-155-?	197	P	32.83	LV	copper	faceted	60.0	9999	-	2	9999	9999	hard to see ice
TB-155-?	198	P	35.44	LV	copper	elongate	87.0	-14.0	2	2	>23.2	>23.2	
TB-155-?	199	P	36.68	LV	copper	irregular	71.0	-15.0	2	2	>23.2	>23.2	
TB-155-?	200	P	42.49	LV	copper	very irregular	126.0	-15.0	2	2	>23.2	>23.2	
TB-155-?	201	P	42.72	LV	copper	irregular	68.0	-23.0	2	2	>23.2	>23.2	
TB-155-?	202	P	59.87	LV	copper	very irregular	75.0	-54.0	1	2	54.9	30.7	
TB-155-?	203	P	65.76	LV	copper	faceted	52.0	-18.0	2	2	>23.2	>23.2	
TB-155-?	204	P	74.18	LV	copper	irregular	71.0	-17.0	2	2	>23.2	>23.2	
TB-155-?	205	P	87.09	LV	copper	very irregular	72.0	-19.0	2	2	>23.2	>23.2	
TB-155-?	206	P	163.10	LV	copper	flat irregular	69.0	-29.0	2	2	>23.2	>23.2	
TB-155-?	207	P	43.48	LV	mineral	irregular	87.0	-34.0	1	2	31.3	26.2	
TB-155-?	208	P	5.21	LV	none	spherical	62.0	-33.0	1	2	30.6	25.9	
TB-155-A1	209	Ps	3.12	LV	none	faceted	83.0	9999	-	1	9999	9999	hard to see ice
TB-155-A1	210	Ps	3.23	LV	none	faceted	81.0	9999	-	1	9999	9999	hard to see ice
TB-155-A1	211	Ps	4.43	LV	none	faceted	112.0	9999	-	1	9999	9999	hard to see ice
TB-155-A1	212	Ps	4.87	LV	none	faceted	83.0	9999	-	1	9999	9999	hard to see ice
TB-155-A1	213	Ps	5.09	LV	none	faceted	86.0	9999	-	1	9999	9999	hard to see ice
TB-155-A1	214	Ps	5.27	LV	none	faceted	110.0	-6.0	1	1	9.2	10.1	
TB-155-A1	215	Ps	5.33	LV	none	elongate	80.0	9999	1	1	9999	9999	
TB-155-A1	216	Ps	5.78	LV	none	faceted	92.0	9999	-	1	9999	9999	hard to see ice

Table 1 continued. Fluid Inclusion Microthermometry Data

FIF	FIID	Origin	Size (µm)	Phases	Solids	Shape	Th (°C)	Tm (°C)	Ice	Stage	NaCl wt%	$CaCl_2$ wt%	Note
TB-155-A1	217	Ps	7.33	LV	none	irregular	84.0	9999	1	1	9999	9999	
TB-155-A1	218	Ps	7.84	LV	none	faceted	85.0	9999	-	1	9999	9999	hard to see ice
TB-155-A1	219	Ps	8.09	LV	none	very irregular	135.0	-6.0	1	1	9.2	10.1	
TB-155-A1	220	Ps	9.22	LV	none	faceted	9999	-5.0	1	1	7.9	8.9	
TB-155-A1	221	Ps	9.47	LV	none	elongate	119.0	9999	-	1	9999	9999	hard to see ice
TB-155-A1	222	Ps	10.12	LV	none	irregular	145.0	-6.0	1	1	9.2	10.1	
TB-155-A1	223	Ps	10.16	LV	none	irregular	95.0	-5.0	1	1	7.9	8.9	
TB-155-A1	224	Ps	11.21	LV	none	irregular	85.0	9999	1	1	9999	9999	
TB-155-A1	225	Ps	11.35	LV	none	irregular	86.0	-6.0	1	1	9.2	10.1	
TB-155-A1	226	Ps	11.38	LV	none	irregular	106.0	9999	-	1	9999	9999	hard to see ice
TB-155-A1	227	Ps	11.99	LV	none	irregular	88.0	-6.0	1	1	9.2	10.1	
TB-155-A1	228	Ps	15.22	LV	none	very irregular	84.0	-5.0	1	1	7.9	8.9	
TB-155-A1	229	Ps	15.25	LV	none	elongate	86.0	-5.0	1	1	7.9	8.9	
TB-155-A1	230	Ps	16.40	LV	none	irregular	86.0	-6.0	1	1	9.2	10.1	
TB-155-A1	231	Ps	17.38	LV	none	irregular	101.0	-5.0	1	1	7.9	8.9	
TB-155-A1	232	Ps	18.12	LV	none	irregular	81.0	-4.0	1	1	6.4	7.5	
TB-155-A1	233	Ps	19.59	LV	none	irregular	85.0	9999	1	1	9999	9999	
TB-155-A1	234	Ps	23.48	LV	none	very irregular	91.0	9999	-	1	9999	9999	hard to see ice
TB-155-A1	235	Ps	41.84	LV	none	irregular	89.0	-6.0	1	1	9.2	10.1	
TB-155-A1	236	Ps	44.19	LV	none	very irregular	146.0	-6.0	1	1	9.2	10.1	
TB-155-A1	237	Ps	54.11	LV	none	very irregular	103.0	-6.0	1	1	9.2	10.1	
TB-155-A14	238	P	12.49	LV	copper	elongate	67.0	-38.0	1	2	34.4	27.3	
TB-155-A14	239	P	20.93	LV	copper	faceted	68.0	-12.0	2	2	>23.2	>23.2	
TB-155-A14	240	P	25.09	LV	copper	irregular	80.0	-10.0	2	2	>23.2	>23.2	
TB-155-A16	241	Ps	3.63	LV	none	faceted	9999	-16.0	1	1	19.4	18.4	
TB-155-A16	242	Ps	3.65	LV	none	faceted	9999	-16.0	1	1	19.4	18.4	
TB-155-A16	243	Ps	3.72	LV	none	faceted	9999	-16.0	1	1	19.4	18.4	
TB-155-A16	244	Ps	4.26	LV	none	faceted	9999	-16.0	1	1	19.4	18.4	
TB-155-A16	245	Ps	4.84	LV	none	faceted	9999	-15.0	1	1	18.6	17.8	
TB-155-A16	246	Ps	5.87	LV	none	faceted	9999	-16.0	1	1	19.4	18.4	
TB-155-A16	247	Ps	6.48	LV	none	faceted	9999	-16.0	1	1	19.4	18.4	
TB-155-A17	248	Ps	4.39	LV	none	faceted	9999	-4.0	1	1	6.4	7.5	
TB-155-A17	249	Ps	5.50	LV	none	faceted	9999	-4.0	1	1	6.4	7.5	
TB-155-A17	250	Ps	6.64	LV	none	faceted	9999	-4.0	1	1	6.4	7.5	
TB-155-A17	251	Ps	6.69	LV	none	faceted	9999	-4.0	1	1	6.4	7.5	
TB-155-A19	252	P	3.72	LV	copper	spherical	57.0	9999	-	2	9999	9999	hard to see ice
TB-155-A19	253	P	4.22	LV	copper	spherical	57.0	9999	-	2	9999	9999	hard to see ice
TB-155-A19	254	P	5.89	LV	copper	spherical	59.0	9999	-	2	9999	9999	hard to see ice
TB-155-A19	255	P	9.57	LV	copper	irregular	91.0	9999	-	2	9999	9999	hard to see ice
TB-155-A19	256	P	10.87	LV	copper	elongate	67.0	-11.0	2	2	>23.2	>23.2	
TB-155-A19	257	P	15.05	LV	copper	spherical	75.0	-11.0	2	2	>23.2	>23.2	
TB-155-A19	258	P	22.95	LV	copper	irregular	69.0	-6.0	2	2	>23.2	>23.2	
TB-155-A19	259	P	24.62	LV	copper	irregular	79.0	9999	2	2	9999	9999	
TB-155-A2	260	Ps	4.27	LV	none	faceted	146.0	-5.0	1	1	7.9	8.9	
TB-155-A2	261	Ps	4.41	LV	none	faceted	100.0	9999	-	1	9999	9999	hard to see ice
TB-155-A2	262	Ps	6.01	LV	none	faceted	138.0	-5.0	1	1	7.9	8.9	
TB-155-A2	263	Ps	6.03	LV	none	elongate	83.0	9999	-	1	9999	9999	hard to see ice
TB-155-A2	264	Ps	6.18	LV	none	faceted	153.0	-5.0	1	1	7.9	8.9	
TB-155-A2	265	Ps	6.35	LV	none	faceted	132.0	-5.0	1	1	7.9	8.9	
TB-155-A2	266	Ps	6.57	LV	none	faceted	150.0	-5.0	1	1	7.9	8.9	
TB-155-A2	267	Ps	6.64	LV	none	faceted	143.0	-5.0	1	1	7.9	8.9	
TB-155-A2	268	Ps	7.58	LV	none	faceted	129.0	-5.0	1	1	7.9	8.9	
TB-155-A2	269	Ps	7.68	LV	none	faceted	135.0	-5.0	1	1	7.9	8.9	
TB-155-A2	270	Ps	9.13	LV	none	faceted	147.0	-5.0	1	1	7.9	8.9	

Table 1 continued. Fluid Inclusion Microthermometry Data

FIF	FIID	Origin	Size (μm)	Phases	Solids	Shape	Th (°C)	Tm (°C)	Ice	Stage	NaCl wt%	$CaCl_2$ wt%	Note
TB-155-A2	271	Ps	10.35	LV	none	faceted	149.0	-5.0	1	1	7.9	8.9	
TB-155-A2	272	Ps	17.95	LV	none	faceted	140.0	-5.0	1	1	7.9	8.9	
TB-155-A2	273	Ps	18.54	LV	none	faceted	89.0	-5.0	1	1	7.9	8.9	
TB-155-A2	274	Ps	19.45	LV	none	faceted	156.0	-5.0	1	1	7.9	8.9	
TB-155-A20	275	P	26.61	L	copper	faceted	<50	-33.0	1	2	30.6	25.9	
TB-155-A20	276	P	9.22	LV	none	faceted	77.0	WNF	-	2	>30.5	>30.5	would not freeze
TB-155-A20	277	P	10.90	LV	none	spherical	63.0	-40.0	1	2	36.1	27.9	
TB-155-A21	278	P	7.67	L	copper	very irregular	<50	-13.0	2	2	>23.2	>23.2	
TB-155-A21	279	P	8.04	LV	copper	spherical	57.0	9999	-	2	9999	9999	hard to see ice
TB-155-A21	280	P	8.10	Lv	copper	elongate	68.0	9999	-	2	9999	9999	
TB-155-A21	281	P	10.17	LV	copper	irregular	82.0	9999	-	2	9999	9999	hard to see ice
TB-155-A21	282	P	15.44	LV	copper	irregular	71.0	9999	-	2	9999	9999	copper broke off
TB-155-A21	283	P	17.31	LV	copper	spherical	62.0	9999	-	2	9999	9999	
TB-155-A21	284	P	38.17	LV	copper	irregular	58.0	-9.0	2	2	>23.2	>23.2	
TB-155-A21	285	P	64.99	LV	copper	elongate	82.0	-11.0	2	2	>23.2	>23.2	
TB-155-A22	286	P	11.13	LV	copper	irregular	66.0	9999	-	2	9999	9999	hard to see ice
TB-155-A22	287	P	11.44	LV	copper	irregular	62.0	9999	-	2	9999	9999	hard to see ice
TB-155-A22	288	P	11.77	LV	copper	irregular	63.0	-11.0	2	2	>23.2	>23.2	
TB-155-A22	289	P	12.08	LV	copper	spherical flat	62.0	-11.0	2	2	>23.2	>23.2	
TB-155-A22	290	P	13.24	LV	copper	elongate	83.0	-10.0	2	2	>23.2	>23.2	copper broke off
TB-155-A22	291	P	16.45	LV	copper	spherical	69.0	-12.0	2	2	>23.2	>23.2	
TB-155-A22	292	P	23.11	LV	copper	elongate	78.0	-11.0	2	2	>23.2	>23.2	
TB-155-A22	293	P	25.08	LV	copper	irregular	60.0	-12.0	2	2	>23.2	>23.2	
TB-155-A23	294	P	4.36	LV	copper	spherical	68.0	9999	-	2	9999	9999	hard to see ice
TB-155-A23	295	P	4.55	LV	copper	irregular	63.0	9999	-	2	9999	9999	hard to see ice
TB-155-A23	296	P	10.35	LV	copper	spherical flat	62.0	WNF	-	2	>30.5	>30.5	would not freeze
TB-155-A23	297	P	14.57	LV	copper	irregular	86.0	9999	-	2	9999	9999	hard to see ice
TB-155-A23	298	P	37.89	LV	copper	irregular	71.0	-11.0	2	2	>23.1	>23.2	
TB-155-A4	299	Ps	14.86	LV	none	faceted	75.0	-6.0	2	2	>23.2	>23.2	
TB-155-A4	300	Ps	17.81	LV	none	spherical	59.0	-6.0	2	2	>23.2	>23.2	
TB-155-A4	301	Ps	20.98	LV	none	faceted	80.0	-6.0	2	2	>23.2	>23.2	
TB-155-A4	302	Ps	21.45	LV	none	faceted	82.0	-7.0	2	2	>23.2	>23.2	
TB-155-A4	303	Ps	22.49	LV	none	faceted	64.0	-6.0	2	2	>23.2	>23.2	
TB-155-A4	304	Ps	23.20	LV	none	faceted	80.0	-6.0	2	2	>23.2	>23.2	
TB-155-A4	305	Ps	25.17	LV	none	faceted	77.0	-6.0	2	2	>23.2	>23.2	
TB-155-A4	306	Ps	26.58	LV	none	faceted	79.0	-7.0	2	2	>23.2	>23.2	
TB-155-A4	307	Ps	28.81	LV	none	faceted	65.0	-7.0	2	2	>23.2	>23.2	
TB-155-A4	308	Ps	28.81	LV	none	faceted	80.0	-6.0	2	2	>23.2	>23.2	
TB-155-A4	309	Ps	34.70	LV	none	spherical	65.0	-7.0	2	2	>23.2	>23.2	
TB-155-A4	310	Ps	38.41	LV	none	irregular	9999	-5.0	2	2	>23.2	>23.2	
TB-155-A4	311	Ps	38.86	LV	none	faceted	64.0	-9.0	2	2	>23.2	>23.2	
TB-155-A8	312	S	9.84	L	none	faceted	<50	-32.0	1	?	30.0	25.5	
TB-155-A8	313	S	12.77	LV	none	faceted	64.0	-32.0	1	?	30.0	25.5	
TB-155-A8	314	S	13.48	LV	none	elongate	77.0	-32.0	1	?	30.0	25.5	
TB-155-A8	315	S	14.61	LV	none	elongate	9999	-31.0	1	?	29.3	25.2	
TB-155-A8	316	S	14.77	LV	none	elongate	61.0	-32.0	1	?	30.0	25.5	
TB-155-A8	317	S	15.57	LV	none	elongate	71.0	-32.0	1	?	30.0	25.5	
TB-155-A8	318	S	17.67	L	none	elongate	<50	-31.0	1	?	29.3	25.2	
TB-155-A8	319	S	26.35	LV	none	faceted	68.0	-32.0	1	?	30.0	25.5	
TB-155-A8	320	S	27.62	LV	none	faceted	75.0	-33.0	1	?	30.6	25.9	
TB-155-A8	321	S	28.09	LV	none	irregular	55.0	-32.0	1	?	30.0	25.5	
TB-155-A8	322	S	34.35	LV	none	spherical	63.0	-32.0	1	?	30.0	25.5	
TB-155-A8	323	S	42.59	LV	none	elongate	80.0	-33.0	1	?	30.6	25.9	
TB-155-A9	324	Ps	6.21	LV	none	faceted	72.0	-32.0	1	2	30.0	25.5	

Table 1 continued. Fluid Inclusion Microthermometry Data

FIF	FIID	Origin	Size (μm)	Phases	Solids	Shape	Th (°C)	Tm (°C)	Ice	Stage	NaCl wt%	$CaCl_2$ wt%	Note
TB-155-A9	325	Ps	7.19	L	none	elongate	<50	-32.0	1	2	30.0	25.5	
TB-155-A9	326	Ps	8.41	LV	none	faceted	73.0	-32.0	1	2	30.0	25.5	
TB-155-A9	327	Ps	8.89	L	none	elongate	<50	-31.0	1	2	29.3	25.2	
TB-155-A9	328	Ps	9.18	LV	none	faceted	64.0	-32.0	1	2	30.0	25.5	
TB-155-A9	329	Ps	11.05	LV	none	faceted	69.0	-32.0	1	2	30.0	25.5	
TB-155-A9	330	Ps	11.81	LV	none	faceted	71.0	-32.0	1	2	30.0	25.5	
TB-155-A9	331	Ps	11.89	LV	none	spherical	64.0	-32.0	1	2	30.0	25.5	
TB-155-A9	332	Ps	11.97	LV	none	elongate	78.0	-32.0	1	2	30.0	25.5	
TB-155-A9	333	Ps	12.21	LV	none	elongate	89.0	-33.0	1	2	30.6	25.9	
TB-155-A9	334	Ps	12.24	LV	none	faceted	72.0	-32.0	1	2	30.0	25.5	
TB-155-A9	335	Ps	14.47	LV	none	faceted	60.0	-32.0	1	2	30.0	25.5	
TB-155-A9	336	Ps	14.66	L	none	irregular	<50	-32.0	1	2	30.0	25.5	
TB-155-A9	337	Ps	14.74	LV	none	faceted	89.0	-32.0	1	2	30.0	25.5	
TB-155-A9	338	Ps	14.82	LV	none	faceted	55.0	-32.0	1	2	30.0	25.5	
TB-155-A9	339	Ps	14.91	LV	none	faceted	61.0	-32.0	1	2	30.0	25.5	
TB-155-A9	340	Ps	15.04	L	none	elongate	<50	-31.0	1	2	29.3	25.2	
TB-155-A9	341	Ps	15.12	LV	none	faceted	72.0	-32.0	1	2	30.0	25.5	
TB-155-A9	342	Ps	15.20	LV	none	elongate	74.0	-32.0	1	2	30.0	25.5	
TB-155-A9	343	Ps	15.87	LV	none	elongate	76.0	-32.0	1	2	30.0	25.5	
TB-155-A9	344	Ps	17.92	LV	none	elongate	74.0	-32.0	1	2	30.0	25.5	
TB-155-A9	345	Ps	17.99	LV	none	faceted	68.0	-32.0	1	2	30.0	25.5	
TB-155-A9	346	Ps	18.65	LV	none	faceted	67.0	-32.0	1	2	30.0	25.5	
TB-155-A9	347	Ps	18.79	LV	none	faceted	59.0	-32.0	1	2	30.0	25.5	
TB-155-A9	348	Ps	20.75	LV	none	elongate	74.0	-32.0	1	2	30.0	25.5	
TB-155-A9	349	Ps	21.54	LV	none	faceted	70.0	-32.0	1	2	30.0	25.5	
TB-155-A9	350	Ps	21.83	L	none	elongate	<50	-32.0	1	2	30.0	25.5	
TB-155-A9	351	Ps	21.86	LV	none	faceted	72.0	-32.0	1	2	30.0	25.5	
TB-155-A9	352	Ps	23.61	LV	none	faceted	75.0	-32.0	1	2	30.0	25.5	
TB-155-A9	353	Ps	24.98	LV	none	faceted	67.0	-32.0	1	2	30.0	25.5	
TB-155-A9	354	Ps	25.98	LV	none	faceted	69.0	-32.0	1	2	30.0	25.5	
TB-155-A9	355	Ps	30.90	LV	none	elongate	73.0	-32.0	1	2	30.0	25.5	
TB-53-A1	356	Ps	4.20	LV	none	spherical	142.0	-8.0	1	2	11.7	12.3	
TB-53-A1	357	Ps	5.20	LV	none	elongate	101.0	9999	-	2	9999	9999	hard to see ice
TB-53-A1	358	Ps	7.58	LV	none	elongate	126.0	-9.0	1	2	12.8	13.3	
TB-53-A1	359	Ps	7.90	LV	none	elongate	73.0	9999	1	2	9999	9999	
TB-53-A1	360	Ps	9.01	LV	none	elongate irregular	73.0	9999	1	2	9999	9999	
TB-53-A1	361	Ps	9.08	LV	none	irregular	74.0	9999	-	2	9999	9999	hard to see ice
TB-53-A1	362	Ps	10.04	LV	none	irregular	133.0	-9.0	1	2	12.8	13.3	
TB-53-A1	363	Ps	10.32	LV	none	irregular	148.0	-8.0	1	2	11.7	12.3	
TB-53-A1	364	Ps	11.36	LV	none	elongate	142.0	-9.0	1	2	12.8	13.3	
TB-53-A1	365	Ps	13.05	LV	none	elongate	149.0	-8.0	1	2	11.7	12.3	
TB-53-A1	366	Ps	13.25	LV	none	irregular	137.0	-9.0	1	2	12.8	13.3	
TB-53-A1	367	Ps	19.75	LV	none	irregular	116.0	-9.0	1	2	12.8	13.3	
TB-53-A1	368	Ps	21.43	LV	none	irregular	103.0	9999	1	2	9999	9999	
TB-53-A1	369	Ps	23.81	LV	none	elongate	133.0	-12.0	1	2	16.0	15.7	
TB-53-A1	370	Ps	26.68	LV	none	elongate	104.0	-11.0	1	2	15.0	15.0	
TB-53-A1	371	Ps	31.01	LV	none	elongate	129.0	-11.0	1	2	15.0	15.0	
TB-53-A2	372	P	7.53	LV	none	irregular	79.0	-26.0	1	3	26.2	23.3	
TB-53-A2	373	P	10.12	LV	none	irregular	59.0	-30.0	1	3	28.7	24.8	
TB-53-A2	374	P	11.05	LV	none	irregular	121.0	-34.0	1	3	31.3	26.2	
TB-53-A2	375	P	11.72	LV	none	irregular	68.0	-28.0	1	3	27.4	24.1	
TB-53-A2	376	P	12.17	LV	none	spherical	53.0	9999	1	3	9999	9999	
TB-53-A2	377	P	12.21	LV	none	irregular	61.0	-51.0	1	3	49.7	30.5	
TB-53-A2	378	P	15.02	LV	none	irregular	9999	-39.0	1	3	35.2	27.6	

Table 1 continued. Fluid Inclusion Microthermometry Data

FIF	FIID	Origin	Size (μm)	Phases	Solids	Shape	Th (°C)	Tm (°C)	Ice	Stage	NaCl wt%	$CaCl_2$ wt%	Note
TB-53-A2	379	P	16.71	LV	none	irregular	9999	-42.0	1	3	38.1	28.4	
TB-53-A2	380	P	17.75	LV	none	irregular	70.0	WNF	-	3	>30.5	>30.5	would not freeze
TB-53-A2	381	P	20.05	LV	none	irregular	9999	-36.0	1	3	32.8	26.8	
TB-53-A2	382	P	22.92	LV	none	irregular	90.0	9999	1	3	9999	9999	
TB-53-A2	383	P	23.28	LV	none	irregular	60.0	-27.0	1	3	26.8	23.7	
TB-53-A2	384	P	28.75	LV	none	very irregular	9999	-34.0	1	3	31.3	26.2	
TB-53-A2	385	P	29.86	LV	none	irregular	61.0	9999	1	3	9999	9999	
TB-53-A2	386	P	31.59	LV	none	irregular	64.0	-39.0	1	3	35.2	27.6	
TB-53-A2	387	P	52.77	LV	none	irregular	9999	-50.0	1	3	48.1	30.3	
TB-53-A2	388	P	73.10	LV	none	very irregular	53.0	-32.0	1	3	30.0	25.5	
TB-53-A2	389	P	81.66	LV	none	very irregular	91.0	-27.0	1	3	26.8	23.7	
TB-53-A2	390	P	88.30	LV?	none	very irregular	9999	-34.0	1	3	31.3	26.2	
TB-53-A3	391	Ps	3.71	-	none	spherical	9999	-3.0	1	3	5.0	5.9	identified post heating
TB-53-A3	392	Ps	4.19	-	none	spherical	9999	-3.0	1	3	5.0	5.9	identified post heating
TB-53-A3	393	Ps	4.34	-	none	spherical	9999	-2.0	1	3	3.4	4.2	identified post heating
TB-53-A3	394	Ps	4.40	-	none	spherical	9999	-3.0	1	3	5.0	5.9	identified post heating
TB-53-A3	395	Ps	4.64	-	none	spherical	9999	-2.0	1	3	3.4	4.2	identified post heating
TB-53-A3	396	Ps	4.74	-	none	spherical	9999	-3.0	1	3	5.0	5.9	identified post heating
TB-53-A3	397	Ps	5.15	-	none	slightly irregular	9999	-3.0	1	3	5.0	5.9	identified post heating
TB-53-A3	398	Ps	5.32	-	none	spherical	9999	-3.0	1	3	5.0	5.9	identified post heating
TB-53-A3	399	Ps	5.47	-	none	spherical	9999	-2.0	1	3	3.4	4.2	identified post heating
TB-53-A3	400	Ps	5.62	-	none	spherical	9999	-2.0	1	3	3.4	4.2	identified post heating
TB-53-A3	401	Ps	5.86	-	none	spherical	9999	-2.0	1	3	3.4	4.2	identified post heating
TB-53-A3	402	Ps	6.16	-	none	elongate	9999	-1.0	1	3	1.7	2.3	identified post heating
TB-53-A3	403	Ps	6.31	-	none	spherical	9999	0.0	1	3	0.0	0.0	identified post heating
TB-53-A3	404	Ps	7.50	-	none	elongate	9999	-3.0	1	3	5.0	5.9	identified post heating
TB-53-A3	405	Ps	7.76	-	none	elongate	9999	-4.0	1	3	6.4	7.5	identified post heating
TB-53-A3	406	Ps	8.34	-	none	spherical irregular	9999	-3.0	1	3	5.0	5.9	identified post heating
TB-53-A3	407	Ps	8.35	-	none	elongate	9999	-3.0	1	3	5.0	5.9	identified post heating
TB-53-A3	408	Ps	9.25	-	none	elongate	9999	-5.0	1	3	7.9	8.9	identified post heating
TB-53-A3	409	Ps	9.88	-	none	elongate	9999	-4.0	1	3	6.4	7.5	identified post heating
TB-53-A3	410	Ps	10.63	-	none	elongate	9999	-2.0	1	3	3.4	4.2	identified post heating
TB-53-A3	411	Ps	12.35	-	none	elongate	9999	-2.0	1	3	3.4	4.2	identified post heating
TB-53-A3	412	Ps	13.06	-	none	irregular elongate	9999	-3.0	1	3	5.0	5.9	identified post heating
TB-53-A3	413	Ps	13.51	-	none	elongate	9999	-4.0	1	3	6.4	7.5	identified post heating
TB-53-A4	414	Ps	6.13	-	none	spherical	9999	-26.0	1	3	26.2	23.3	identified post heating
TB-53-A4	415	Ps	6.16	-	none	slightly irregular	9999	-25.0	1	3	25.6	22.9	identified post heating
TB-53-A4	416	Ps	6.22	-	none	spherical	9999	-25.0	1	3	25.6	22.9	identified post heating
TB-53-A4	417	Ps	6.33	-	none	spherical	9999	-25.0	1	3	25.6	22.9	identified post heating
TB-53-A4	418	Ps	6.69	-	none	spherical	9999	-25.0	1	3	25.6	22.9	identified post heating
TB-53-A4	419	Ps	7.48	-	none	spherical	9999	-26.0	1	3	26.2	23.3	identified post heating
TB-53-A4	420	Ps	8.44	-	none	spherical	9999	-26.0	1	3	26.2	23.3	identified post heating
TB-53-A4	421	Ps	8.49	-	none	spherical	9999	-25.0	1	3	25.6	22.9	identified post heating
TB-53-A4	422	Ps	8.94	-	none	spherical	9999	-26.0	1	3	26.2	23.3	identified post heating
TB-53-A4	423	Ps	9.76	-	none	spherical	9999	-25.0	1	3	25.6	22.9	identified post heating
TB-53-A4	424	Ps	9.85	-	none	spherical	9999	-25.0	1	3	25.6	22.9	identified post heating
TB-53-A4	425	Ps	11.59	-	none	spherical	9999	-26.0	1	3	26.2	23.3	identified post heating
TB-53-A4	426	Ps	11.69	-	none	elongate	9999	-26.0	1	3	26.2	23.3	identified post heating
TB-53-A4	427	Ps	19.29	-	none	irregular elongate	9999	-28.0	1	3	27.4	24.1	identified post heating
TB-53-A5	428	Ps	6.00	-	none	faceted?	9999	-21.0	1	3	23.0	21.1	identified post heating
TB-53-A5	429	Ps	6.20	-	none	elongate	9999	-21.0	1	3	23.0	21.1	identified post heating
TB-53-A5	430	Ps	6.45	-	none	elongate	9999	-21.0	1	3	23.0	21.1	identified post heating
TB-53-A5	431	Ps	6.85	-	none	elongate	9999	-20.0	1	3	22.4	20.6	identified post heating
TB-53-A5	432	Ps	7.04	-	none	spherical	9999	-20.0	1	3	22.4	20.6	identified post heating

Table 1 continued. Fluid Inclusion Microthermometry Data

FIF	FIID	Origin	Size (µm)	Phases	Solids	Shape	Th (°C)	Tm (°C)	Ice	Stage	NaCl wt%	$CaCl_2$ wt%	Note
TB-53-A5	433	Ps	7.66	-	none	elongate	9999	-21.0	1	3	23.0	21.1	identified post heating
TB-53-A5	434	Ps	7.96	-	none	elongate	9999	-21.0	1	3	23.0	21.1	identified post heating
TB-53-A5	435	Ps	8.16	-	none	spherical	9999	-21.0	1	3	23.0	21.1	identified post heating
TB-53-A5	436	Ps	8.29	-	none	elongate	9999	-21.0	1	3	23.0	21.1	identified post heating
TB-53-A5	437	Ps	8.61	-	none	elongate	9999	-21.0	1	3	23.0	21.1	identified post heating
TB-53-A5	438	Ps	8.67	-	none	spherical	9999	-21.0	1	3	23.0	21.1	identified post heating
TB-53-A5	439	Ps	9.19	-	none	spherical	9999	-21.0	1	3	23.0	21.1	identified post heating
TB-53-A5	440	Ps	9.28	-	none	irregular	9999	-20.0	1	3	22.4	20.6	identified post heating
TB-53-A5	441	Ps	9.64	-	none	elongate	9999	-21.0	1	3	23.0	21.1	identified post heating
TB-53-A5	442	Ps	12.77	-	none	elongate	9999	-21.0	1	3	23.0	21.1	identified post heating
TB-53-A5	443	Ps	14.33	-	none	elongate	9999	-22.0	1	3	23.7	21.5	identified post heating
TB-53-A5	444	Ps	16.46	-	none	elongate	9999	-20.0	1	3	22.4	20.6	identified post heating
TB-53-A6	445	Ps	4.99	-	none	spherical	9999	-36.0	1	3	32.8	26.8	identified post heating
TB-53-A6	446	Ps	5.02	-	none	spherical	9999	-36.0	1	3	32.8	26.8	identified post heating
TB-53-A6	447	Ps	5.64	-	none	elongate	9999	WNF	-	3	>30.5	>30.5	identified post heating
TB-53-A6	448	Ps	6.10	-	none	elongate	9999	-36.0	1	3	32.8	26.8	identified post heating
TB-53-A6	449	Ps	6.66	-	none	elongate	9999	-36.0	1	3	32.8	26.8	identified post heating
TB-53-A6	450	Ps	6.71	-	none	spherical	9999	-37.0	1	3	33.6	27.1	identified post heating
TB-53-A6	451	Ps	7.22	-	none	elongate	9999	-37.0	1	3	33.6	27.1	identified post heating
TB-53-A6	452	Ps	7.82	-	none	elongate	9999	-37.0	1	3	33.6	27.1	identified post heating
TB-53-A6	453	Ps	8.67	-	none	elongate	9999	-37.0	1	3	33.6	27.1	identified post heating
TB-53-A6	454	Ps	8.86	-	none	elongate	9999	-36.0	1	3	32.8	26.8	identified post heating
TB-53-A6	455	Ps	9.68	-	none	elongate	9999	-37.0	1	3	33.6	27.1	identified post heating
WAS323-2-A1	456	P	6.60	LV	none	faceted	66.0	-33.0	1	2	30.6	25.9	
WAS323-2-A1	457	P	6.79	LV	none	faceted	64.0	-33.0	1	2	30.6	25.9	
WAS323-2-A1	458	P	9.18	LV	none	faceted	62.0	-33.0	1	2	30.6	25.9	
WAS323-2-A1	459	P	9.32	LV	none	faceted	9999	-33.0	1	2	30.6	25.9	
WAS323-2-A1	460	P	9.89	LV	none	faceted	49.0	-33.0	1	2	30.6	25.9	
WAS323-2-A1	461	P	10.86	LV	none	faceted	62.0	-33.0	1	2	30.6	25.9	
WAS323-2-A1	462	P	11.38	LV	none	faceted	62.0	-33.0	1	2	30.6	25.9	
WAS323-2-A1	463	P	11.49	LV	none	faceted	63.0	-33.0	1	2	30.6	25.9	
WAS323-2-A1	464	P	11.97	LV	none	faceted	66.0	-33.0	1	2	30.6	25.9	
WAS323-2-A1	465	P	11.98	LV	none	faceted	65.0	-33.0	1	2	30.6	25.9	
WAS323-2-A1	466	P	12.01	LV	none	faceted	44.0	-33.0	1	2	30.6	25.9	
WAS323-2-A1	467	P	12.99	LV	none	faceted	62.0	-33.0	1	2	30.6	25.9	
WAS323-2-A1	468	P	14.88	LV	none	faceted	64.0	-33.0	1	2	30.6	25.9	
WAS323-2-A1	469	P	20.70	LV	none	irregular	78.0	-39.0	1	2	35.2	27.6	
WAS323-2-A1	470	P	28.88	LV	none	irregular	68.0	-33.0	1	2	30.6	25.9	

Explanation: **FIF** = fluid inclusion family, the first part half of the number shows the thick section and the number after the "A" represents what fluid inclusion family within that thick section it belongs to; **FID** = fluid inclusion identifier number, this is a sequential number used to identify individual fluid inclusions; **Origin** = interpretation of how the fluid inclusion formed based on petrography, primary (P), pseudosecondary (Ps), secondary (S); **Size(µm)** = size of fluid inclusion measured along longest dimension; **Phases** = phases present in the fluid inclusion at room temperature before microthermometry, L = liquid, LV = liquid and vapor, - = no observation was made before microthermometry; **Solids** = indicates if a fluid inclusion was in contact with a

solid other than calcite, native copper (copper), another mineral (mineral), or none; **Shape** = basic description of fluid inclusion shape, (faceted) = inclusions that had a negative crystal shape, (elongate) = inclusions that had a length at least twice as long as width, (spherical) = inclusions that were nearly equal in all dimensions, (flat) = inclusions that appeared blade like or disc shaped, (irregular) = inclusions that did not fit any easily recognized shape, these terms could be further used in conjunction with "slightly" or "very" or used together for a better description of inclusion shape; **Th(°C)** = homogenization temperature, 9999 = tested but no usable data was obtained; **Tm(°C)** = final melting temperature, (WNF) = would not freeze, 9999 = tested but no usable data was obtained; **Ice** = number of solid phases present with low temperature microthermometry, - = not determined; **NaCl equiv. wt. %** = an estimate of salinity in equivalent NaCl weight percent; **$CaCl_2$ equiv. wt. %** = an estimate of salinity in equivalent $CaCl_2$ weight percent; **Note** = special observation of fluid inclusion, (would not freeze) = the inclusion did not produce a solid phase at low temperatures, (identified post heating) = the inclusion had already been heated by the time it was discovered leaving only low temperature microthermomtry possible, (hard to see ice) = the solid phases produced at low temperatures were too difficult to observe, (hard to see bubble) = the vapor phase was too difficult to observe during microthermometry, (copper broke off) = during microthermomtry experiments the native copper became separated from the calcite and became totally immersed in the fluid inclusion.